Přírodovědecká fakulta
Faculty of Science

Jihočeská univerzita v Českých Budějovicích
University of South Bohemia in České Budějovice

Bachelor Thesis

Localization of the F_1-ATP Synthase Subunit α and its N‘ and C‘ Terminal Fragments in *Trypanosoma brucei* Cells

Laboratory of Molecular Biology of Protists
Institute of Parasitology
České Budějovice, 2018

Leonie Lehmayer

Supervisor: RNDr. Alena Panicucci Zíková, PhD

Co-supervisor: Brian Panicucci

Lehmayer, L., 2018: "Localization of the F_1-ATP Synthase Subunit α and its N‘ and C‘ Terminal Fragments in *Trypanosoma brucei* cells" Bachelor of Science Thesis, Faculty of Science, University of South Bohemia, České Budějovice, Czech Republic

Annotation

In this thesis, we explored if the proteolytically excised octapeptide from the *Trypanosoma brucei* F_1-ATP synthase subunit α can act as a mitochondrial targeting sequence. Three procyclic 29.13 *T. brucei* cell lines were generated to express tagged variants of the α subunit. We then determined where these heterologous proteins were localized within the parasite. This preliminary data provides insights about where the α subunit proteolytic cleavage events occur within the cell.

Declaration

I hereby declare that I have worked on the submitted bachelor thesis independently and used only the sources listed in the bibliography.

I hereby declare that, in accordance with Article 47b of Act No. 111/1998 in the valid wording, I agree with the publication of my bachelor thesis, in full form to be kept in the Faculty of Science archive, in electronic form in publicly accessible part of the STAG database operated by the University of South Bohemia in České Budějovice accessible through its web pages.

Further, I agree to the electronic publication of the comments of my supervisor and thesis opponents and the record of the proceedings and the results of the thesis defence in accordance with aforementioned Act No. 111/1998. I also agree to the comparison of the text with the Thesis.cz thesis database operated by the National Registry of University Theses and a plagiarism detection system.

České Budějovice, ……. ……

Leonie Lehmayer

Acknowledgement

I would like to thank Alena for providing me the great opportunity to work in her lab, it was truly an amazing experience. A big thank you also to Brian for his never-ending patience, support and guidance during the whole process of this thesis.

Abbreviations

ADP	Adenosine diphosphate
APRT	Adenine phosphoribosyltransferase
APS	Ammonium persulfate
ATOM	Archaic translocases of the outer membrane
ATP	Adenosine triphosphate
BF	Bloodstream form
BN	Blue native
BSA	Bovine serum albumine
Cyto	Cytosolic
DNA	Deoxyribonucleic acid
dNTP	Deoxynucleotide
DTE	Dithioerythritiol
EDTA	Ethylenediaminetetraacetic acid
EtBr	Ethidium bromide
ETC	Electron transport chain
FBS	Fetal bovine serum
G	Neomycin
gDNA	genomic DNA
H	Hygromycin
HRP	Horseradish peroxidase
Hsp	Heatshock protein
IFA	Immunofluorescence assay
IM	Inner membrane
IMS	Inner membrane space
kDa	Kilodalton
LB	Lysogeny Broth
mNG	mNeonGreen
mNTS	Mitochondrial N-terminal targeting sequence

mt	Mitochondrial
nt	Nucleotides
OM	Outer membrane
organ	Organic
P	Puromycin
PAGE	Polyacrylamide gel electrophoresis
PBS	Phosphate buffered saline
PCR	Polymerase chain reaction
PF	Procyclic form
PVDF	Polyvinylidene fluoride
RNA	Ribonucleic acid
RNAi	RNA interference
rDNA	Ribosomal DNA
RT	Room temperature
SDS	Sodium dodecyl sulfate
TAO	Trypanosome alternative oxidase
TEMED	Tetramethylethylenediamine
TIM	Translocases of the inner membrane
TMRE	Tetramethylrhodamine, ethyl ester
UTR	Untranslated region
WCL	Whole cell lysates

Table of Contents

1. Introduction

1.1 Trypanosoma brucei

1.1.1 Human Parasite, Disease, Life Cycle

Trypanosomatids are single-flagellated protists of the class Kinetoplastida, belonging to the supergroup Excavata. This group of medically significant parasites is comprised of three human pathogens: *Trypanosoma brucei, T. cruzi* and *Leishmania* (Kaufer et al., 2017). In particular, the species *T. brucei* is a model organism of Kinetoplastida because its genome is easily manipulated by forward and reverse genetics (Matthews, 2015). *T. brucei* is heteroxenous, requiring a vertebrate and an invertebrate host to complete one full life cycle. Since the available nutrients in the insect host (tsetse fly) and the mammal host vary to a great extent, this organism must rapidly adapt its morphology and metabolism as it transitions between two completely different environments (Smith et al., 2017). Therefore, the parasite cycles between two distinct life stages, the bloodstream form (BF) in the mammal host and the procyclic form (PF) in the tsetse fly (Figure 1). While the life cycle is quite complex in nature, typically only the BF and PF trypomastigotes can easily be cultivated to high densities in the lab. Recent advances now also allow for the in vitro differentiation of the parasite to both life stages (Kolev et al., 2012).

The *T. brucei* subspecies *Trypanosoma brucei gambiense*, found in west and central Africa, is responsible for more than 98% of reported Human African trypanosomiasis (HAT), also known as sleeping sickness. These pathogens cause chronic infections, whereas the subspecies *Trypanosoma brucei rhodiense* in eastern and southern Africa is responsible for an acute infection that progresses rapidly within weeks after infection (Simarro et al., 2010; Babokhov et al., 2013). To avoid the risk of infection when working with this organism in the laboratory, the subspecies *T. brucei brucei* is often used because it is susceptible to a human lytic factor. Therefore, it only infects cattle and other livestock (Tomlinson and Raper, 1996).

The clinical progression of HAT is divided into two stages. During the hemolymphatic phase (Stage I), the parasite is localized in the blood and lymphatic system of the carrier. This infection manifests in mild flu-like symptoms, which are often misdiagnosed and the patient is often treated incorrectly (Simarro et al., 2012). The parasites are then able to cross the blood-brain barrier and infect the central nervous system during the neurological or meningo-

encephalic stage (Stage II). The symptoms of stage II are far more severe and include disturbances in the sleeping cycle of the patient, which gives the disease its name. Other symptoms include confusion, disturbance of the senses and changes in the patient's behaviour (Büscher et al., 2017). If the disease stays untreated, it is highly likely to lead to death; however, cases of self-cure after infection by *T. brucei gambiense* have been reported (Jamonneau et al., 2012).

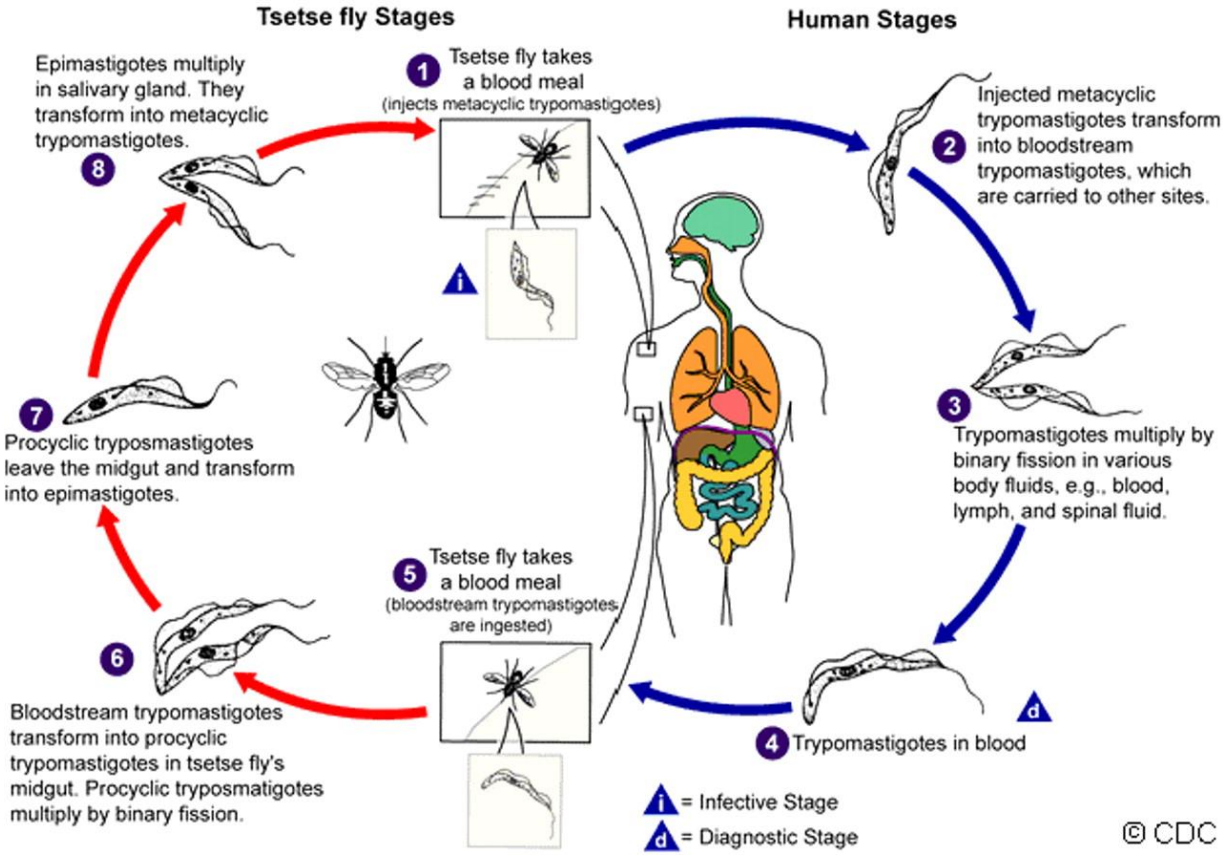

Figure 1 - A mammal becomes infected when a tsetse fly haboring metacyclic trypomastigotes takes a blood meal (1). Inside the mammalian bloodstream, the extracellular parasite adapts its morphology as it transitions into a long slender bloodstream form (BF) (2). These flagellated protists replicate by binary fission (3) and can occupy body fluids throughout the body (4). The life cycle continues when a tsetse fly ingests the bloodstream trypomastigotes, which are transported to the midgut (5). Due to the new environment, the parasites transform into procyclic forms (PF) and again replicate by binary fission (6). As they leave the fly's midgut, they transform into epimastigotes (6) before they reach the fly's salivary glands. Here they replicate again by binary fission and transform into metacyclic trypamastigotes (8). (Image source: Centers for Disease Control and Prevention, Parasites - African Trypanosomiasis – Biology; Information courtesy to DPDx; https://www.cdc.gov/parasites/sleepingsickness/biology.html; date of access: 14.07.2018)

1.1.2 Changes in Metabolism Between Life Stages

1.1.2.1 Procyclic Form

The environment of the tsetse fly's midgut is low in glucose, but high in amino acids. Therefore, like many eukaryotes, most of the cellular demands for ATP are generated by the mitochondrion. Unlike most eukaryotes though, *T. brucei* has only a single reticulated mitochondrion that occupies most of the cell body (Verner et al., 2015). Within the cristae micro-environment of the mitochondrial (mt) inner membrane (IM), the enzymatic complexes of the electron transport chain (ETC) accept electrons from NADH or $FADH_2$ and use this energy to pump protons into the intermembrane space (IMS). The high energy molecules $FADH_2$ and NADH are synthesized by the catabolism of specific amino acids, which are mainly proline, glutamine and threonine. As in a typical ETC, the electrons primarily enter via various dehydrogenases. Respiratory complex I harnesses the energy from the oxidation of NADH to drive proton pumping from the matrix into the IMS. In contrast, the transfer of electrons from reduced $FADH_2$ to complex II does not result in the translocation of any protons. The electrons from complex I and II are then transferred to the cytochrome bc1 complex (complex III) via the fat-soluble coenzyme Q_{10}. The energy released as the electrons cascade down complex III on their way to cytochrome c is once again used to pump protons into the IMS. Finally, the water-soluble hemeprotein cytochrome c transfers its electron to cytochrome c oxidase (complex IV). Protons are once more pumped into the IMS as oxygen is used as the final electron acceptor and is reduced to water (Verner et al., 2015).

Due to the change in proton concentration across the IM, a membrane potential is generated. The combination of the proton gradient and the membrane potential result in the proton motive force (PMF) (Dimroth et al., 1999). Because of the establishment of the PMF, protons want to run down their gradient and return to the matrix where the concentration of ions is lower. Therefore, the final step in the oxidative phosphorylation pathway involves the F_oF_1-ATP synthase. Protons pass through a pore in this rotary enzyme so that the potential energy of the proton gradient is transformed into a rotational mechanical energy that creates chemical energy in the form of ATP (Walker, 2013). Since the PF parasite residing in the midgut of the tsetse fly relies on the catabolism of available amino acids, the resulting NADH and FADH feed electrons into the oxidative phosphorylation pathway to generate most of the cellular demand for ATP.

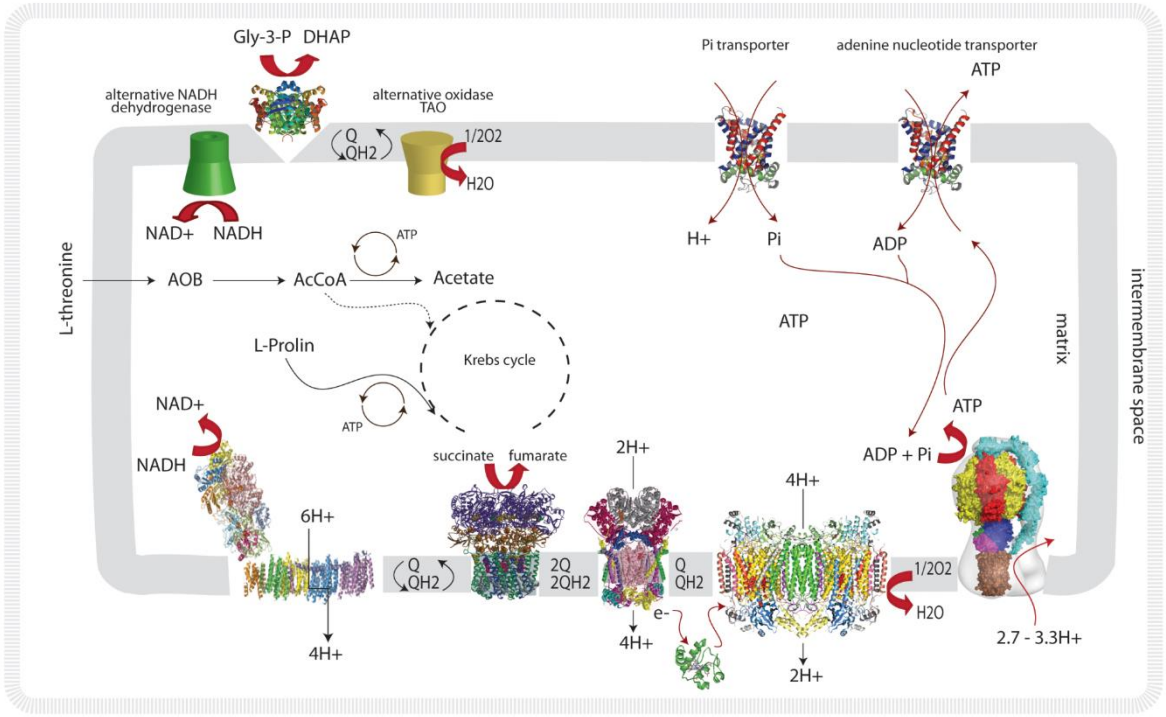

Figure 2 – Schematic picture of the PF mitochondrial metabolism including the respiratory chain and F_OF_1-ATP synthase needed for oxidative phosphorylation. (Zíková laboratory rendering of the PF mitochondria)

1.1.2.2 Bloodstream Form

When this extracellular parasite occupies the bloodstream of the mammalian host, energy production relies solely on glycolysis, as there is an excess of glucose in the blood. The first enzymatic steps of glycolysis occur in peroxisome-like organelles called glycosomes. Glycosomes are unique organelles that have only been found in species of Kinetoplastida. During the metabolism of glucose to pyruvate, the first seven glycolytic enzymes are found in the BF glycosome (Blattner, 1998). The last step to occur in the glycosome is the creation of ATP and 3-phosphoglycerate by phosphoglycerate kinase. Interestingly, this enzyme is localized in the cytosol of the PF parasite, but the cytosolic expression of phosphoglycerate kinase in BF cells is toxic. This presumably occurs because it competes for the glycosomal substrate and prevents full ATP regeneration in the BF glycosome, inhibiting the essential first steps of glycolysis (Gualdron-Lopez et al., 2012).

After the catabolism of glucose to 3-phosphoglycerate, the final degradation steps to pyruvate occur in the cytosol of the BF *T. brucei*. Pyruvate is the most prominent end product of glycolysis, although traces of succinate, alanine and acetate are also excreted (Mazet, 2013). The electrons produced from the oxidation of glycolytic substrates are transferred to oxygen in the mitochondrion. However, the BF mitochondrion lacks a cytochrome-mediated respiratory chain and most of the Krebs cycle enzymes. Therefore, they utilize a glycerol-3-phosphate shuttle that passes electrons from the glycosome to a mt glycerol-3-phosphate dehydrogenase. Within the mitochondrion, the electrons are then passed to ubiquinone and finally to the trypanosome alternative oxidase, TAO (Chaudhuri et al., 2006). Since there in no proton pumping associated with this pathway, no electrochemical gradient is formed and there is no linkage to ATP production. Since a mitochondrial membrane potential is essential for mt protein import, the ATP synthase works in reverse by hydrolysing ATP to ADP and inorganic phosphate. This provides the mechanical energy required to pump protons into the mt inner membrane space (Schnaufer et al., 2005).

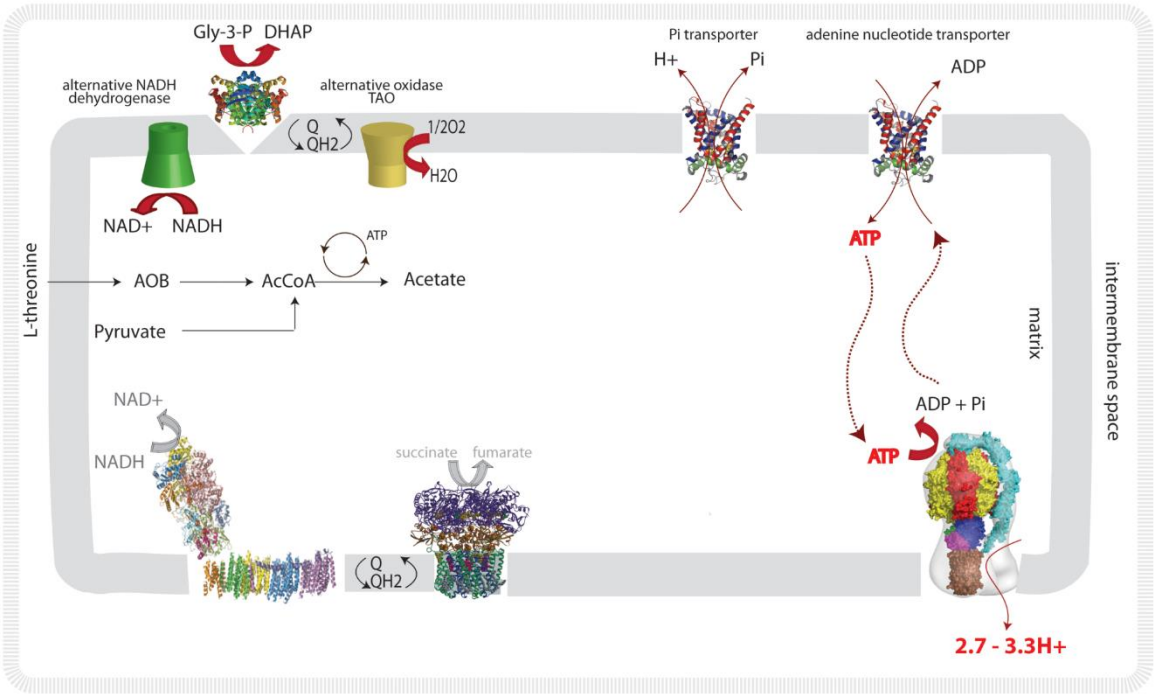

Figure 3 – Schematic picture of the reduced mitochondrial metabolism in BF compared to PF cells (Figure 2). The Krebs cycle and the cytochrome-mediated respiratory chain are lacking, thus the F_OF_1-ATP synthase works in reverse. (Zíková laboratory rendering of the BF mitochondria)

1.2 The ATP synthase

ATP synthases are enzyme complexes that generate ATP in bacteria, chloroplasts and mitochondria. The composition of mitochondrial F_oF_1-ATP synthases can vary between organisms, but the overall architecture and mechanism is highly conserved across life-forms. This multisubunit complex consists of two functional domains, a membrane intrinsic F_O domain and a membrane extrinsic F_1 domain that protrudes into the mt matrix. The eukaryotic F_1 domain (Figure 4) consists of the subunits α, β, γ, δ, ε with a stoichiometry of $\alpha_3\beta_3\gamma_1\delta_1\varepsilon_1$. The α and β subunits assemble to form a hexamer with alternating α and β subunits. The structures of α and β subunits are similar, each consisting of three different domains: an N-terminal domain, a central domain and a C-terminal domain. Nucleotide binding at the central domain of subunit β plays a catalytical role, whereas nucleotide binding to the α subunit serves a regulatory role. The catalytical F_1 head group that synthesizes ATP from ADP and inorganic phosphate is connected to the membrane embedded F_O domain by the central stalk, subunit γ. The F_O domain is comprised of subunit a, the c-ring consisting of 8-12 copies of subunit c and the peripheral stalk (Figure 4). Subunits b, d, F6 and OSCP form the peripheral stalk that extends from subunit a in the mt inner membrane to the top of the F_1 αβ-hexamer (Walker, 2013).

The synthesis of ATP relies on the electrochemical gradient formed when the ETC pumps protons into the IMS. These protons then flow down their concentration gradient by passing through a proton pore created between the c-ring and subunit a of the F_oF_1-ATP synthase. The protons bind to acidic amino acid residues situated on the c subunits, therefore neutralizing them. The neutralized residue then moves to the more hydrophobic environment inside the membrane, causing the c-ring to rotate and expose the next free c subunit that can bind a proton. The protons are then released into the mitochondrial matrix due to the pH difference (pH=8), resulting in a negatively charged amino acid residue that can then be protonated again. As the F_O c-ring rotates, it propels the attached central stalk to move clockwise as seen from the bottom (membrane embedded Fo domain) of the enzyme. Meanwhile the catalytic αβ-hexamer is held stationary by the peripheral stalk. Since subunit γ is asymmetrical, this rotary mechanism leads to conformational changes in each αβ-dimer, providing the impetus for the synthesis of ATP from ADP and inorganic phosphate. Each 120° degree turn of the gamma subunit causes an αβ dimer to undergo three different conformations. These stages are described based on the catalytic status of subunit β, as β_{DP} binds ADP, β_{TP}

binds ATP and β_E releases ATP (Klusch et al., 2017). Hence, the formation of an ATP molecule starts with the binding of ADP and inorganic phosphate to subunit β to induce a loose β_{DP} state. As the central stalk rotates, the conformation changes to the tighter β_{TP} conformation, leading to the formation of one ATP molecule. Finally, ATP is then released when the open β_E conformation is obtained by an additional rotation of γ. Therefore, each complete rotation of 360° leads to one ATP molecule formed by each αβ dimer, resulting in a total of three ATP molecules produced (Walker, 2013).

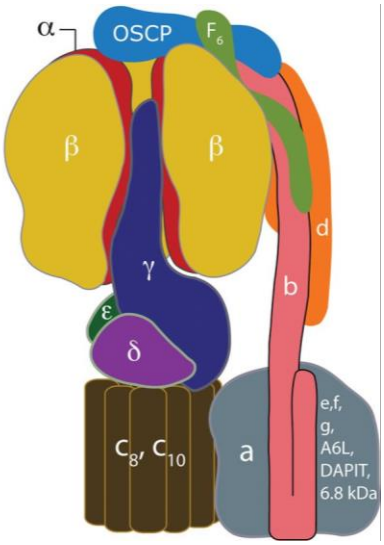

Figure 4 – A schematic picture of a eukaryotic mitochondrial ATP synthase, showing the subunits of the F_1 domain: the αβ-hexamer (α in red and β in yellow), γ (the central stalk, in dark purple) with the associated subunits δ (in purple) and ε (in dark green). The subunits of the F_O domain consist of: c subunits forming a ring (in brown), subunit a (in grey) and subunits of the peripheral stalk: subunit b (pink), d (orange), F_6 (green) and OSCP (blue). Image adapted from Walker, 2013

1.3 Unique Attributes of the T. brucei ATP Synthase

Since trypanosomatids are an evolutionary early-branching organism, they have accumulated a number of unique biological properties. The *T. brucei* F_oF_1-ATP synthase complex is another example of how diverse life-forms converge to solve essential life problems in a similar way, but with some notable twists. For example, the mass spectrometry analysis of the *T. brucei* F_OF_1-ATP synthase isolated by a tandem affinity purification revealed that its composition was unique. 22 proteins were determined to comprise the parasitic enzyme, but

only five homologs of F_1 (α, β, γ, δ, ε) and three homologs of F_O (a, c and OSCP) were identified. The remaining 14 proteins have no known homologs outside Euglenozoans (Zíková et al., 2009). Either these *T. brucei* subunits are highly diverged from other eukaryotes or they are new proteins that are examples of convergent evolution. One of these unique subunits, p18, was recently shown to be an addition to the previously considered highly conserved F_1 structure. Furthermore, RNAi silencing demonstrated that this euglenozoan specific subunit is essential for the stability of the F_1-ATPase in BF *T. brucei*. While p18 contains two pentatricopeptide repeat (PPR) motifs that are often associated with RNA metabolism in mitochondria, chloroplasts and some bacteria species, the true function of this subunit is still unknown (Gahura et al., 2017; Montgomery et al., 2018).

Another unique feature of the *T. brucei* ATP synthase involves the proteolytic cleavage of the α subunit into a 13 kDa N-terminal peptide and a 47 kDa C-terminal peptide (Figure 5). Both α peptides remain bound to the assembled ATP synthase complex. While this proteolytic event has been observed in other euglenozoan organisms before, the cleavage site and the resulting mature peptides had not been precisely identified until recently. Using mass spectrometry of the biochemically purified enzymatic complex, the molecular weights of the two α protein fragments were determined and it was revealed that there are two internal cleavage sites that excise an octapeptide. Each cleavage site is preceded by a leucine residue at positions 151 and 159 (Gahura et al., 2017). There has been no evidence to suggest that the α fragmentation results in a less stable complex (Montgomery et al., 2018). However, it has not been determined if this cleavage is necessary for proper *T. brucei* ATP synthase activity. Furthermore, the responsible protease(s) has not yet been identified.

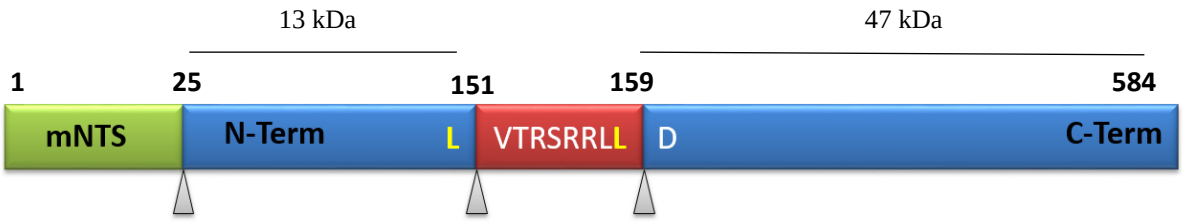

Figure 5 – Schematic representation of the full length (FL) α protein. The green bar represents the mitochondrial N-terminal targeting sequence (mNTS), the blue bars represent the two α fragments (N-terminal and C-terminal) resulting from the two additional proteolytic events. The cleavage sites are indicated by the grey triangles and the excised octapeptide is represented by the red bar. The leucine residues immediately upstream of both cleavage sites are highlighted in yellow.

1.4 Mitochondrial Protein Import in *T. brucei*

While the morphology and function of the BF *T. brucei* mitochondrion is reduced, it still performs functions that are essential to parasite survival. Since more than 95% of the mitochondrial proteins are nuclear encoded, they must be efficiently transported into the mitochondrion (Peikert et al., 2017). The transportation and integration of proteins into the mitochondria depends on the type and structure of the proteins. The import machinery of *T.brucei* includes the archaic translocases of the outer membrane (ATOM) and translocases of the inner membrane (TIM). The ATOM complex consists of seven subunits (Mani et al., 2015; Desy et al., 2016), which is similar to the TOM complex in yeast, but only two *T. brucei* homologs have been identified (Mani et al., 2016). Furthermore, compared to the three TIM complexes identified in yeast, *T. brucei* might only contain a single TIM complex with compositional variations that help to sort carrier proteins into the IM and proteins with a mitochondrial N-terminal targeting sequence (mNTS) into the matrix (Gentle et al., 2007; Schneider et al., 2008; Eckers et al., 2012). ATOM is a general protein translocase that is capable of importing a wide variety of proteins into the IMS, including beta barrel proteins, carrier proteins, proteins of cysteine rich motifs (such as Cx_3C motifs of tiny TIM chaperones) and proteins containing an mNTS. After translocation into the IMS, the very hydrophobic beta barrel proteins probably first interact with tiny TIM chaperones before being embedded into the outer membrane by the sorting and assembling machinery (SAM). In the case of a small IMS protein containing a cysteine rich motif, the import is likely mediated by either Erv1 proteins alone or with the help of other yet unidentified enzymes since the homolog of Mia40 has not been determined (Basu et al., 2013; Eckers et al., 2013; Allen et al., 2008). If the imported protein contains a mNTS or is a mitochondrial carrier protein, it gets transported to the TIM complex located in the IM with the help of tiny TIM chaperones. During the translocation event, the TIM complex undergoes conformational changes that either inserts the protein into the IM or releases it into the mitochondrial matrix (Harsman, 2016).

1.5 The Mitochondrial N-Terminal Targeting Sequence

Since the ATOM and TIM complexes interact with the mNTS, it is presumed that they arose during evolution to increase the import specificity of mt matrix proteins. It has been

suggested that a positively charged mNTS arose already in the eukaryotic common ancestor to make use of the membrane potential across the IM and get electrophoretically imported into the matrix (Garg et al., 2015). In addition to the membrane potential, the TIM complex requires a typically ATP-mediated motor in order to translocate proteins from the IMS into the matrix (Schulz et al., 2015). The *T. brucei* orthologues to the yeast PAM motor were identified as subunits Tim44, Pam18 and the mitochondrial heat shock protein mHSP70 (Schneider et al., 2008). Finally, the mitochondrial processing peptidase (MPP) in the matrix then cleaves off the mNTS to produce the mature protein (Mach, 2013).

While most nuclear-encoded matrix proteins contain an mNTS, some mature matrix proteins lacking a mNTS have been identified. For example, the mature F_oF_1-ATP synthase γ subunit does not contain a processed mNTS (Gahura et al, 2017). Thus, these proteins must contain an internal sequence that targets the protein to the organelle (Neupert et al., 2007). Often the starting methionine of these proteins is cleaved and the second amino acid, usually an alanine or serine (Carroll et al., 2005), is acetylated. This is the case with the *T. brucei* γ subunit. Another example involves the mt import of the *T. brucei* alternative oxidase (TAO) (Hamilton et al., 2014). The removal of the predicted mNTS did not result in any import alterations in vitro, leading to the conclusion that the protein sequence must contain an extra internal targeting sequence. Indeed, an in silico Mitoprot analysis suggested a possible internal targeting sequence. This internal targeting sequence was then fused with the cytosolic protein dihydrofolate reductase (DHFR) and the in vivo mt import was monitored. Surprisingly, the internal targeting sequence showed better efficiency of mt import than the control DHFR fused with the predicted TAO mNTS.

2. Aims of the Thesis

The aims of this thesis include the following:

- Clone three F_1-ATP synthase α subunit variants into a V5 tagged trypanosome protein expression vector
- Analyse the localization of these heterologous proteins within the cell by subcellular fractionation
- Verify the subcellular localization of these tagged α subunits by performing an immunofluorescence assay
- Determine whether the V5 tagged protein is successfully incorporated into the F_OF_1-ATP synthase complex

3. Materials and Methods

3.1 Cloning

The purpose of this project was to express three variants of the *T. brucei* F_oF_1-ATP synthase α subunit (TriTrypDB gene ID: Tb927.7.7420) in PF *T. brucei* and determine where they were localized within the cell. Therefore, we chose to clone the α subunit variants into a regulatable *T. brucei* protein expression plasmid (pT7-3V5-PAC) that fuses a 3x V5 epitope tag to the C-terminus of the protein.

3.1.1 PCR

Three different DNA segments of the *T. brucei* F_oF_1-ATP synthase α subunit were amplified by PCR:

i) "Full length α" (FL α) is the whole protein coding sequence, including the known mitochondrial targeting sequence at the beginning of the N-terminus

ii) "N-terminal" (N-term) encodes the α peptide starting from the defined mitochondrial targeting signal and extending until the first internal cleavage site that removes an octapeptide from the mature protein

iii) "C-terminal + 8" (C-Term +8) begins from the first internal cleavage site and extends the entire length of the coding sequence. Thus, the 5' end of the amplicon encodes for the octapeptide that is cleaved from the mature α subunit.

To amplify these different sequences, four primers were designed using the software Geneious (Table 1). The primer annealing sites on subunit α are schematically visualized in Figure 6.

Table 1 – Primers designed to amplify gene fragments of interest, start codons (ATG) are indicated by bold letters, restriction site sequences are indicated by underlined letters.

Name	Amplicon	Forward Primer	ID	Reverse Primer	ID
FL α	1-584	CGCAAGCTT**ATG**CGT CGCT	1	ACAGGATCCCACTGCC CGCTTA	3
N-term	1-151	CGCAAGCTT**ATG**CGT CGCT	1	ATAGGATCCGAGCCCC ACCGGAA	4
C-term + 8	152-584	CGCAAGCTT**ATG**GTT ACCCGCAGTC	2	ACAGGATCCCACTGCC CGCTTA	3

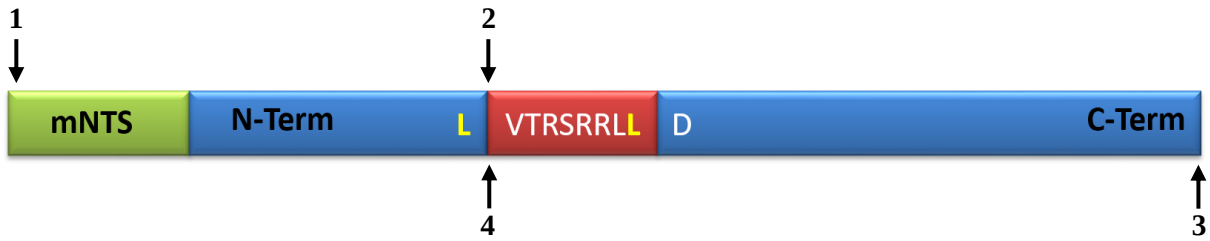

Figure 6 – Schematic picture of subunit α. The arrows mark the annealing sites of the primers (primer ID numbers 1, 2, 3, 4 according to Table 1).

The forward primers contain a start codon (ATG) that encodes for methionine whereas the stop codon was excluded from the reverse primers, allowing for the in-frame fusion of the C-terminal V5 epitope. The forward primers also included a HindIII (AAGCTT) restriction sites, while the reverse primer contained a BamHI (GGATCC) restriction site. Finally, three nonspecific nucleotides were added to the 5' end of each primer so the restriction enzymes had enough DNA to bind without falling off the end. This helps with the digestion efficiency of the amplicons so they can be directly cloned into the final vector.

Previously isolated genomic DNA (gDNA) from *T. brucei* cells was used as the template for the PCR. To limit the number of errors introduced into the amplicons, the proofreading polymerase AMPOne Fast Pfu from GeneAll was used. To ensure enough of each amplicon was generated for subsequent cloning, two PCR reactions were performed in the reaction mixtures described in Table 2.

Table 2 – PCR reaction mixture (50 µL)

Reagent	[Stock]	Vol (µL)	[Final]
gDNA	100 ng/µL	1	100 ng
MilliQ		35	
Fast-Pfu Buffer (7.5mM Mg^{2+})	5x	10	1x
dNTP	10 mM	1	0.2 mM
Forward Primer	0.1 mM	1	2 µM
Reverse Primer	0.1 mM	1	2 µM
AMPOne Fast-Pfu polymerase		1	1 U

The PCR program was run according to Table 3, with 30 cycles of the denaturing, annealing and extension steps.

Table 3– PCR program

Step	Temp (°C)	Time	Cycles
PCR activation	98	30 sec	
Denaturation	98	30 sec	30
Annealing	53	20 sec	
Extension	72	40 sec	
Final extension	72	5 min	

3.1.2 Gel Electrophoresis and Extraction

To verify whether the PCR successfully amplified a single band of the expected size, the PCR products were analysed by agarose gel electrophoresis. The 50 µL PCR samples were mixed with 6 µL of 10x DNA loading dye (Table 4) containing 0.1% xylene cyanol to track the progress of the DNA migration and 39% glycerol to help the samples sink into the wells of a 1% agarose gel. The gel was prepared by dissolving 7 g of agarose powder in 70 mL of boiling 1x TAE electrophoresis buffer (Table 5). The hot agarose solution was allowed to cool slightly before 1 µL of 10 mg/mL ethidium bromide (EtBr) was added to visualize the DNA bands in the gel under UV-light. Gel Electrophoresis was performed at 100 volts for 1 hour. To determine the size of the PCR products, a 1kb Plus DNA ladder from GeneRuler was loaded

next in the first well of the gel. Subsequently the gel was visualized using the ChemiDoc MP imaging system and the software ImageLab.

The expected sized PCR bands were then excised from the gel by following the instruction manual for the Gel Extraction Kit provided by Sigma-Aldrich. Briefly, the bands of DNA were visualized on a transilluminator equipped with a long-wavelength (302 nm) UV light source and then excised from the gel with a clean razor blade. The gel slices were solubilized by the addition of three gel volumes of the gel solubilization solution (300 µL/100 mg). These samples were then incubated at 60°C for 10 minutes (min) to completely dissolve the gel into a homogenous solution. Isopropanol was then added and the solutions were transferred to binding columns that were previously equilibrated with a preparation solution that enhances the binding capacity of the spin column's membrane. The spin columns were washed and the DNA was eluted with elution buffer heated to 65°C. The concentrations and 260/280 ratios of the eluted DNA were determined using the Thermo-Fisher Nanodrop spectrophotometer.

Table 4 – 10x DNA loading dye (10 mL)

Reagent	[Stock]	10 mL	[Final]
MilliQ		4.2 mL	
Glycerol	80%	4.9 mL	39%
SDS	10%	500 µL	0.5%
EDTA	0.5 M	200 µL	10 mM
Xylene cyanol	2%	250 µL	0.1%

Table 5 – 1x TAE electrophoresis buffer, pH 8.0 (1 L)

Reagent	[Stock] / Molecular Weight	1 L	[Final]
MilliQ		900 mL	
Trizma base	121.14 g/mol	4.84 g	40 mM
Glacial acetic acid	60.05 g/mol	1.1 mL	20 mM
EDTA, pH 8.0	0.5 M	2 mL	1 mM

3.1.3 Digestion of Amplicons

For efficient and directional cloning into the final vector, the PCR products need to be digested with restriction enzymes. Based on the multiple cloning site of the target vector, we selected which restriction digest recognition sequences to include in the primers used to synthesize our amplicons. Thus, our amplicons were incubated in a 37°C heating block for 1 hour with the Fast Digest restriction enzymes BamHI and HindIII (Thermo Fisher Scientific). These enzymes create 5' overhangs (Figure 7) or sticky ends that will anneal with the complementary base pairs from another DNA molecule (vector) digested with the same enzyme. Reaction mixtures were created as stated in Table 6.

BamHI **HindIII**

5' – G | G A T C C - 3' 5' - A | A G C T T - 3'
3' – C C T A G | G - 5' 3' - T T C G A | A - 5'

Figure 7 – Restriction enzyme recognition sites

Table 6 – Amplicon digestion reaction mixture (100µL)

Reagent	Vol (µL)
Amplicon	60
10x Fast Digest Buffer	10
BamHI	2
HindIII	2
MilliQ	26

Afterwards, the digestion reactions were treated with the GenElute PCR Clean-up kit (Sigma-Aldrich) to prepare them for downstream cloning procedures. As described in the instruction manual, this kit helps to remove the enzymes, change the buffer and remove the small nucleotide tails digested from the ends of the amplicon. Briefly, the digest reactions were transferred to a binding column, washed and finally eluted with elution buffer warmed to 65°C. The obtained DNA concentrations and 260/280 ratios were again determined using the Thermo-Fisher Nanodrop spectrophotometer.

3.1.4 Preparing the Plasmid for Cloning

Depending on the type of experiment to be performed, it is crucial to choose a suitable plasmid. We chose to work with the trypanosome protein expression vector, pT7-3V5-PAC (Figure 8 and 9) because it contained the following required properties:

i) our gene of interest is preceded by a T7 RNA polymerase promoter sequence that is recognized by the heterologous T7 polymerase that is constitutively expressed in PF *T. brucei* 29.13 cells

ii) the transcription of our gene can be regulated (turned on or off) because of the *T. brucei* heterologous expression of a tetracycline repressor that binds to a DNA element situated between the T7 promoter and our gene

iii) our gene product will be fused in frame at the C-terminal end with 3x V5 epitope tags that can be used to track protein expression by western blot analysis

iv) genomic integration of the regulatable gene product will occur at the *T. brucei* rDNA spacer region by homologous recombination

v) positive selection of the transformed/transfected plasmid into *E. coli/T. brucei* is possible due to the presence of selectable markers against the antibiotics ampicillin (*E. coli*) and puromycin (*T. brucei)*

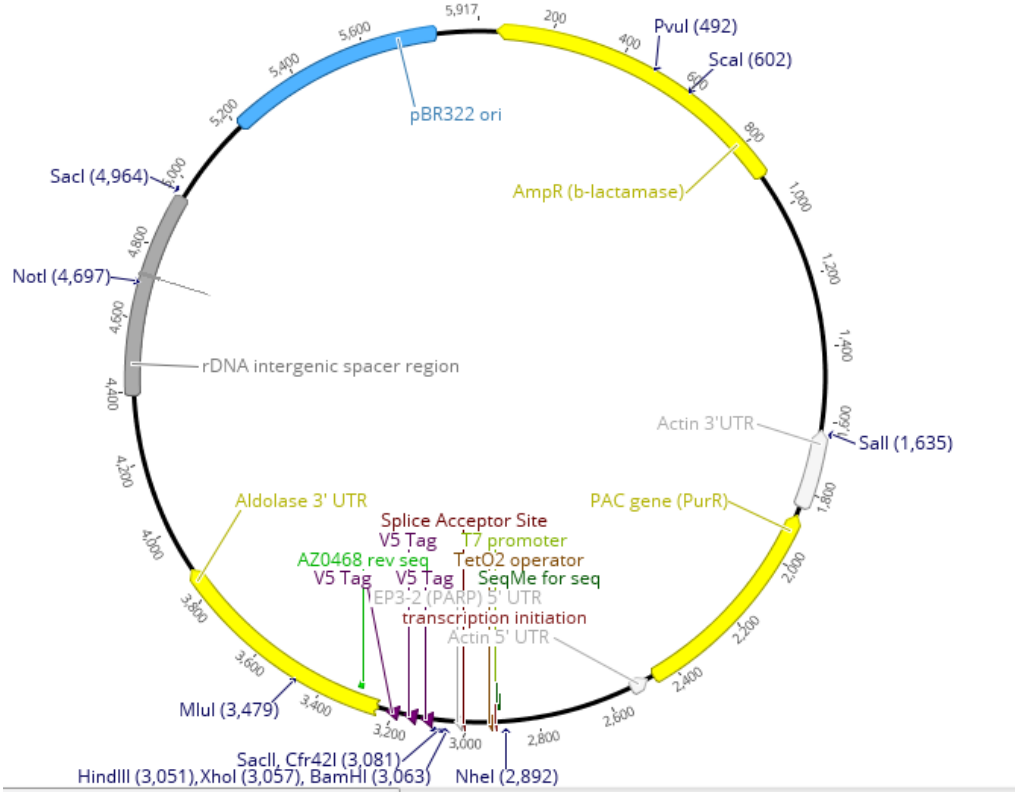

Figure 8 – Schematic overview of the protein expression plasmid pT7-3V5-PAC.

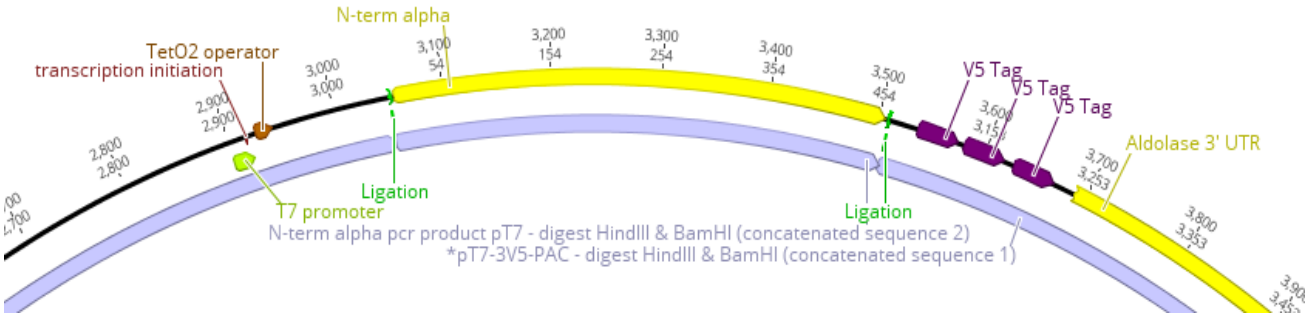

Figure 9 – Close up of the plasmid with ligated N-term shown as an example. The T7 promoter and Tetracycline operator can be seen upstream of the insert, the 3x V5 tags are situated downstream at the C-terminus of the inserted DNA.

To create the complementary sticky ends for each of the α amplicons, the vector was incubated with BamHI and HindIII for 30 min at 37°C. The reaction mixture was set up as stated in Table 7. When the digestion was completed, 5 µL of 10x DNA loading dye were added and the digested vector was resolved on an 1% agarose gel. The linearized DNA band of the expected size was then excised from the gel. These procedures were carried out as described in section 3.1.2.

Table 7 – pT7-3V5-PAC digestion reaction mixture (50 µL)

Reagent	Volume (µL)
MilliQ	36.8
10xFD Green Buffer	5.0
Plasmid (10 µg)	4.2
HindIII	2.0
BamHI	2.0

3.1.5 Ligation

Once complementary sticky ends from two DNA molecules anneal, a DNA ligase is required to form two covalent phosphodiester bonds between the 3' hydroxyl end of one acceptor nucleotide with the 5' phosphate end of another donor molecule. Since intramolecular ligations are more likely to occur than between two DNA molecules, we need to incubate the smaller amplicon with the larger vector backbone in a 3:1 molar ratio. Below (Figure 10) is the equation used to calculate the molarity of each DNA molecule (Table 8). The DNA ligations were performed with a T4 DNA ligase (Promega) supplied with a 10x ligase buffer. Since the reactions should be limited to 10 µL and it is optimal to have ~100 ng of total DNA, we formulated the following ligation reactions (Table 9). These were then incubated at 4°C overnight.

$$\text{nM} = \frac{DNA\ concentration_{insert}\ [ng/\mu L]}{0.325\ [g/mol] * number\ of\ bp} * 10^3$$

Figure 10 – equation used for the calculation of the molarity of each DNA molecule

Table 8 – Calculated molarity (nM) of plasmid and α inserts

DNA molecule	Conc. (ng/µL)$^-$	Length (nt)	Molarity (nM)
pT7-3V5-PAC	103.4	5909	54.0
FL α	13.4	1752	24.0
N-Term	17.1	453	116.0
C-Term + 8	56.2	1296	133.4

Table 9 – T4 DNA ligation reactions (10 µL)

Reagent	FL α (µL)	N-Term (µL)	C-Term + 8 (µL)
MilliQ	-	5.5	5.75
10x Ligase Buffer	1	1	1
Plasmid	1	1	1
Insert	7	1.5	1.25
T4 Ligase	1	1	1

3.2 Transformation into *Escherichia coli*

3.2.1 Transformation

To obtain a higher quantity of the recombinant plasmid, the ligation mixture was transformed into the chemically competent *Escherichia coli* strain XL-1 blue. A 50 µL aliquot of the competent cells was thawed on ice for 20 min before 3 µL of each ligation reaction were added. The Eppendorf tube was gently flicked to mix the contents without disrupting the fragile competent bacteria. The bacteria were then incubated with the DNA on ice for 20 min before they were induced to take up the foreign DNA by shocking them with heat (42°C) for 45 seconds. The bacteria were then allowed to recover on ice for 2 min before 250 µL of sterile SOC medium (Table 10) was added. The nutrient rich SOC medium helps to maximize the transformation efficiency. The bacteria were then incubated at 37°C in a shaking incubator for 45 min to encourage cell growth. After this step, 250 µL of the transformed cells were spread onto a petri plate containing Lysogeny broth (LB) agar (Table 11 with 15 g of agar added). To select for bacteria that contained our plasmid, positive selection was performed by the addition of 100 µg/mL of the ampicillin antibiotic to the LB agar. The LB agar was created with a lower salt (NaCl) concentration because the selective antibiotic is salt sensitive. The plates were incubated at 37°C for approximately 14 hours to limit the opportunities for satellite colony growth. Thus, the resulting *E. coli* colonies should contain the plasmid that expresses the selectable marker that can degrade ampicillin.

Table 10 – SOC medium

Component	Amount (g/L)
Tryptone	20.00
Yeast Extract	5.000
$MgSO_4$	4.800
Dextrose	3.603
NaCl	0.500
KCl	0.186

Table 11 – LB medium (1L)

Reagent	MW (g/mol)	[Final]	Amount
MilliQ			800 mL
Tryptone		1%	10 g
Yeast Extract		0.5%	5 g
NaCl	58.44	85 mM	0.5 g
Filled up with MilliQ to:			**1000 mL**

3.2.2 GenElute HP Plasmid Miniprep

To determine if the positively selected bacterial clones contain the plasmid with the correct insert, we need to isolate the plasmid DNA. Therefore, overnight cultures of four individual colonies from each transformation plate were replica plated and used to inoculate a 5 mL LB culture (Table 11) containing 5 µL of 100 mg/mL ampicillin. Those cultures were incubated for 14 hours at 37°C on a shaking incubator at 200 rotations per minute (rpm).

The cells of the overnight recombinant *E. coli* culture were harvested by centrifugation at 12,000*g for 1 min and the supernatant was decanted. The protocol provided by the GenElute HP Plasmid Miniprep Kit by Sigma-Aldrich was then followed. Briefly, the cells were resuspended and subsequently lysed by the addition of a lysis buffer. After a 5 min incubation, a neutralization buffer was added to prevent further lysis. Cell debris, proteins, lipids, SDS and chromosomal DNA fell out of the solution as a cloudy, white viscous precipitate. The mixture was spun down (12,000*g for 10 min) and the cleared lysate solution was carefully pipetted off and transferred to a binding column. The spin column was then washed twice before the plasmid DNA was eluted with previously heated elution buffer. The

concentration and 260/280 ratio of the eluted DNA was determined using the Thermo-Fisher Nanodrop Spectrophotometer.

3.2.3 Plasmid Verification

To determine whether the isolated plasmid DNA is correct, 1 µg of plasmid DNA was digested with the same restriction enzymes used to clone the amplicon into the vector. The digest reactions were set up as listed in Table 12. After incubation for one hour at 37°C, the digests were resolved on a 1% agarose gel and compared to a 1kb Plus DNA ladder. Visualization of the resulting DNA bands stained with EtBr suggested which clone should be sent for sequencing (SeqMe, Czech Republic). The T7 promoter region of our plasmid was utilized for the forward sequencing reaction, while a specific oligo made to the *T. brucei* aldolase 3' UTR, which is situated downstream of the 3x V5 tags, was used for the reverse reaction. Both primer binding sites are part of the vector backbone and thus could be used to sequence the α subunit inserts in all three plasmids (FL α, N-term and C-term + 8 pT7-3V5-PAC). Both the forward and reverse sequencing reactions were necessary to cover the complete coding sequencing of the FL α subunit (~2,000 nt). To identify any errors introduced to the α subunit during the cloning steps, the obtained DNA sequences were then aligned to the corresponding in silico molecule generated in the software program Geneious.

Table 12 – Digestion reaction mixtures (50 µL)

Component	**FL α (µL)**				**N-term (µL)**				**C-term + 8 (µL)**		
Clone	1	2	3	4	1	2	3	4	1	2	3
MilliQ	37.7	41.5	41.7	42.1	41.5	41.3	40.5	41.6	41.7	41.7	41.7
10xFD Buffer	5	5	5	5	5	5	5	5	5	5	5
BamHI	1	1	1	1	1	1	1	1	1	1	1
HindIII	1	1	1	1	1	1	1	1	1	1	1
Plasmid (1 µg)	5.3	4.5	4.3	3.9	4.5	4.7	5.5	4.4	4.3	4.3	4.3

3.2.4 Midiprep and Linearization

The PF *T. brucei* transfection protocol requires 10-12 µg of linearized plasmid DNA. Therefore, sufficient amounts of the plasmid were isolated from bacteria using the GenElute midiprep kit (Sigma Aldrich). This procedure is similar to the Miniprep kit (section 3.1.2), but utilizes 10x more bacteria. To increase the efficiency of the transfected DNA to be integrated into the genomic DNA of the parasite, the plasmid must first be linearized. Therefore, the plasmid was digested with NotI because its palindromic recognition sequence was engineered to occur just once within the plasmid, specifically in the middle of the *T. brucei* rDNA spacer region. This generates a linearized molecule with ends that are available for homologous recombination into the rDNA spacer region of the parasite. Each restriction digest was performed as outlined in Table 13 and incubated at 37°C for 3 hours.

Table 13 – Digestion reaction (50 µL)

Reagent	FL α (µL)	N-Term (µL)	C-Term + 8 (µL)
Plasmid (20µg)	18.3	5.1	5.5
MilliQ	21.7	34.9	34.5
10x FD buffer	5.0	5.0	5.0
NotI	5.0	5.0	5.0

The linearized plasmid was then precipitated by adding 1/10 of the DNA's volume of 3 M Sodium Acetate (pH 5.2) and 2.5 volumes of 97% ethanol. After vortexing, they were incubated at -80°C for 30 min. Centrifugation at 4°C for 30 min at maximum speed was performed. The obtained cell pellet was washed with 200 µL of 70% Ethanol. The DNA was then resuspended in the tissue culture hood with 30 µL sterile distilled water preheated to 65°C. The concentration and 260/280 ratio was determined using the Thermo-Fisher Nanodrop Spectrophotometer. A small amount of each linearized plasmid was run next to the uncut plasmid on a 0.8% agarose gel to verify the efficiency of the linearization process.

3.3 Transfection

3.3.1 Transfection via Electroporation

To perform in vivo experiments, the linearized pT7-3V5-PAC vectors containing the three different alpha mutants were transfected into PF *T. brucei* 29-13 cells. This specific strain contains genes that encode for a T7 RNA polymerase and a Tetracycline repressor, both of which are used for regulatable heterologous protein expression. Each of these ectopic genes were transfected with selectable markers that allowed for the positive selection of parasites that could grow in the presence of the antibiotics neomycin (G) and hygromycin (H). This cell line was thawed from liquid nitrogen stabilates provided by the laboratory. They were cultured in SDM-79 media supplemented with 10% fetal bovine serum (FBS) and the antibiotics G/H (final concentration G: 15 µg/mL; H: 25 µg/mL). The cell cultures were grown in a 27°C incubator. As soon as the cells reached a normal growth rate, growing from a cell density of $1x10^6$ cells/mL to $1x10^7$ cells/mL in two days, they were harvested to carry out the transfection via electroporation using the BTX ECM 630.

To increase the transfection efficiency of *T. brucei*, the cell culture needs to be growing at mid-log phase, usually between 4-8$x10^7$ cells/mL. The cell density was measured using the Z2 Coulter Counter and $1x10^8$ cells were harvested for two transfections of each alpha mutant by spinning the cell culture at 1,300*g for 10 min at 4°C. The media was decanted and the cell pellets were washed with a precooled cytomix buffer (Table 14) and then resuspended in 1 mL cytomix buffer. Four 0.2 cm gap cuvettes were prepared by loading 12 µg of linearized DNA for either 1) FL α, 2) N-terminal, 3) C-terminal + 8 or a 4) mock transfection with no DNA. Next, 0.5 mL of the resuspended PF 29.13 cells were added to each cuvette and subsequently electroporated using the BTX ECM 630 machine with the settings mentioned in Table 15.

Table 14 – Cytomix buffer preparation (100 mL)

Reagent	[Stock]	[Final]	Amount for 100 mL
MilliQ			80 mL
Hepes (pH 7.6)	2 M	25 mM	1.25 mL
KCl	2 M	120 mM	6 mL
$CaCl_2$	1 M	0.15 mM	15 µL
Potassium Phosphate Buffer (pH 7.6)	0.1	10	10 mL
EDTA	0.5	2	400 µL
$MgCl_2$	1	5	500 µL
Glucose		6	0.1 g

Table 15 – Electroporation settings

Applied	Amount
Voltage	1600 V
Resistance	25 Ω
Capacity	50 µF

After electroporation, the cells were immediately resuspended in 6 mL SDM-79 media containing 10% FBS and the antibiotics G/H. Using a microscope, it was confirmed that the parasites were still alive and moving. After incubation at 27°C for 16 hours, another 6 mL of SDM-79 with 10% FBS and the antibiotics G/H were added to the cells, but this time the selectable antibiotic puromycin (P) was added in a 2x concentration (2 µg/mL). 2 mL of the transfected cells were then plated into the first row (A) of a 24 well plate. The plates consisted of four rows (A, B, C, D) and 6 columns (1 to 6). 1.5 mL of SDM-79 with 10% FBS and the antibiotics G/H/P was added to the wells in rows B and C, while only 1 mL was added to the wells of row D. Then serial dilution was performed by transferring 0.5 mL of the cells from row A into row B, where they were thoroughly mixed by pipetting up and down. Then 0.5 mL of cells from row B were transferred into row C and mixed well before finally transferring 0.5 mL into row D. This allowed us to select wells of transfected cells that originated from the least dense populations.

After performing the serial dilution, the cells were kept incubated at 27°C for 8-10 days, until the cultures were growing densely enough to start splitting. The general rule followed for this was: when the bottom of the well becomes completely full of cells, split them 1:1 into a new well. If the cells recover well and are again very dense the following day, split them 1:3 into a new well. Once the well becomes very dense again, split them 1:5. After two days of growth, the well should be very dense again. Then transfer 1 mL of cells to a 25 cm^2 TC flask and add 4 mL of fresh media. Once the cells conditioned the new flask, they should be split 1:10 every two days in a volume of 10 mL total. Once the cells are growing at a regular rate and had been split several times, liquid nitrogen stocks were created.

3.3.2 Protein Expression

As already mentioned, PF 29.13 cells constitutively express a tetracycline repressor that binds to the tetracycline operator located between the T7 promoter and our α subunit variants. This physically blocks the T7 RNA polymerase from transcribing the introduced gene. To turn on this ectopic gene expression, 1 µg/mL of the antibiotic tetracycline was added to the culture. In the cell, tetracycline binds the tetracycline repressor and causes a conformational change that releases it from the DNA.

3.3.2.1 Harvesting Whole Cell Lysates

To determine if the selected cell lines were capable of inducible expression of the heterologous protein, a western blot was performed using whole cell lysates (WCL) prepared from tetracycline induced cells and non-induced cells as a control. WCL were prepared from $1x10^8$ cells. The cell density of each culture was counted and the cells were centrifuged at 1,300*g for 10 min at 12°C. The media was quickly decanted into a bucket with bleach and the cells were immediately placed on ice to prevent the activation of proteases that may have been released from any lysed cells. The cell pellets were resuspended in 1 mL 1x PBS-G (Table 17), transferred into an Eppendorf tube and spun down at 1,300*g for 10 min at 4°C. After aspirating out the supernatant, the cells were resuspended in 200 µL 1x PBS (prepared from 10x PBS, Table 16) and 100 µL 3x SDS-PAGE loading dye. These volumes were calculated so that 30 µL of the WCL would represent about $1x10^7$ cells. The protein samples were then

denatured by incubating in a 97°C heat block for 7 min. For longer term storage, the samples were subsequently stored at -20°C.

Table 16 – 10x PBS (1 L)

Reagent	Molecular weight (g/mol)	[Final]	Amount for 1 L
MilliQ			900 mL
$Na_2HPO_4•12H_2O$	358.14	0.10 M	35.8 g
$NaH_2PO_4•2H_2O$	156.01	0.10 M	15.6 g
NaCl	58.44	1.5 M	85.0 g
Filled up with MilliQ to:			**1000 mL**

Table 17 - PBS-G (500 mL)

Reagent	[Stock] / Molecular weight	]Final]	Amount for 500 mL
MilliQ			450 mL
PBS	10x	1x	50 mL
Glucose	180.16 g/mol	6 mM	0.514 g

3.3.2.2 Western Blot

In order to detect our V5 tagged protein from all the other T. brucei proteins, the WCL needs to be resolved on a polyacrylamide gel. We prepared our own gels with a 5% stacking gel and a 10% resolving gel (Table 18). The gels were run in a 1x SDS running buffer (prepared from 10x SDS running buffer, Table 19) and the PageRuler Prestained Protein Ladder was loaded to determine the apparent molecular weight of the detected proteins. 30 µL ($1x10^7$ cell equivalents) of each WCL was loaded and the gel was run at 90 V until the loading dye reached the resolving gel, then the voltage was increased to 110 V. As soon as the dye reached the bottom of the resolving gel, the applied voltage was stopped.

Table 18 – Gel preparations, amounts for 1 gel

Reagent	5% Stacking gel	10% Resolving gel
MilliQ	1.7 mL	2.4 mL
30% acrylamide mix	420 µL	2 mL
1M Tris (pH 6.8)	315 µL	-
1M Tris (pH 8.8)	-	1.5 mL
10% SDS	25 µL	60 µL
10% APS	25 µL	60 µL
TEMED	5 µL	6 µL

Table 19 – 10x SDS running buffer

Reagent	Molecular weight (g/mol)	[Final]	Amount for 1L
MilliQ			700 mL
Tris	121.14	250 mM	30.3 g
Glycine	75.07	1.92 M	144.4 g
SDS	280.4	1%	10 g
Filled up with MilliQ to:			**1 L**

While the gel was running, the blotting material was prepared. The PVDF membrane (Pall) was first activated by immersing it into methanol for 40 seconds, then washing it in MilliQ for 2 min and finally equilibrating it with 1x transfer buffer (prepared from 10x transfer buffer, Table 20) for at least 5 min. The blotting paper and sponges were also soaked in 1x transfer buffer.

Table 20 - 10x Transfer buffer

Reagent	Molecular weight (g/mol)	[Final]	Amount for 1L
MilliQ			700 mL
Tris	121.14	480 mM	58.15 g
Glycine	75.07	390 mM	29.27 g
Filled up with MilliQ to:			1 L

When the SDS-PAGE was finished, the gel was carefully removed from the glass plates and submersed in 1x transfer buffer. The layers of the blotting sandwich were compiled, the transfer tank was filled with 1x transfer buffer and 90 V were applied for 90 min. The blotting

layers were carefully disassembled and the transfer efficiency was estimated by how much of the prestained protein ladder remained in the gel. If a significant amount remained the transfer should be prolonged. The membrane was then carefully transferred into a 50 mL falcon tube and filled with 45 mL of 5% skim milk in 1x PBS-T (Table 21) to block the membrane. The casein rich milk blocks the membrane by covering it indiscriminately with proteins, thus limiting the interactions of the applied antibody to any unspecific proteins. The membrane was rotated at room temperature (RT) for 1 hour and then incubated at 4°C overnight. The next day, the tube was rotated again at RT for additional 15 min.

Table 21 – 1x PBS-T

Reagent	Molecular weight (g/mol)	[Final]	Amount for 5 L
MilliQ			4500 mL
10xPBS		1x	500 mL
Tween 20	1227.72	0.05%	2.5 mL
Filled up with MilliQ to:			5 L

3.3.2.3 Probing and Visualization

The western blots were first probed with a monoclonal mouse anti-V5-antibody that was diluted 1:2000 in 5 mL of 5% milk. The anti-V5 antibody recognizes and binds the V5 epitope in each of the tagged α subunit proteins. The membrane was incubated with the primary antibody for 1 hour at RT on a rotating platform. The milk and antibody were then decanted and the membrane was briefly rinsed with 1x PBS-T. The membrane was then washed once with 25 mL 1x PBS-T for 15 min and finally washed two times with 25 mL 1x PBS-T for 5 min. Next, a polyclonal goat anti-mouse antibody with horseradish peroxidase (HRP) covalently attached was diluted 1:2000 in 5 mL of 5% milk. The membrane was again incubated with the secondary antibody for 1 hour at RT. Afterwards the same washing procedure with 1x PBS-T was performed as before. To visualize the proteins, the HRP substrate Clarity ECL reagent (BioRad) was mixed in a 1:1 ratio and incubated with the blots for 1 min. Excess liquid was drained by capillary action onto a paper towel and the membrane was placed between two plastic sheets. The membrane was then inspected using the Chemidoc instrumentation running the software ImageLab.

3.3.3 Subcellular Localization

To determine where the α subunit variants are expressed in the cell, a crude but reproducible subcellular fractionation was performed using digitonin and differential centrifugation. This resulted in a cytosolic fraction and an organellar fraction that contained mitochondria, nuclei, glycosomes, golgi, etc. WCL samples were compared to the equivalent amounts of cytosolic and organellar fractions and specific cytosolic and mitochondrial markers were used to verify the purity of the subcellular fractions. Whole cell lysates were prepared as previously described in 3.3.2.1.

For each subcellular fractionation, $1x10^8$ induced cells were harvested by spinning at 1,300*g for 10 min at 4°C. The cell pellet was resuspended in 1.0 mL 1x PBS-G, transferred to a 1.5 mL Eppendorf tube and spun again. The supernatant was carefully aspirated and the cell pellet was thoroughly resuspended in 500 µL SoTE (Table 22) by pipetting up and down several times. Next, 500 µL of a SoTE/0.03% digitonin mixture was added to the cell suspension and the tube was inverted just once before being placed on ice for 5 min. The sample was then spun at 7,000 rpm for 3 min at 4°C. The cytosolic supernatant fraction (~1 mL) was carefully transferred to a new Eppendorf tube and the organellar pellet was resuspended in a volume of SoTe buffer that was equal to the volume of the supernatant (~1 mL). From these two fractions, 100 µL were transferred into a new tube and 50 µL of 3x SDS-PAGE dye were added. The samples were boiled at 97°C for 7 min in a heating block and then stored at -20°C for longer storage.

Table 22 – SoTE solution preparation

Reagent	[Stock] / Molecular weight	[Final]	Amount for 50 mL
MilliQ			40 mL
Tris-HCl, pH 7.5	1 M	20 mM	1 mL
Sorbitol	182.2 g/mol	0.6 M	5.47 g
EDTA	0.5 M	2 mM	200 µL
Filled up with MilliQ to:			50 mL

The western blot was carried out as previously described in section 3.3.2.2. Since these results will likely be part of a manuscript, we used the 4-20% Mini-PROTEAN TGX Stain-

Free precast gels (BioRad) to ensure reproducibility between samples. Furthermore, these gradient gels are capable of resolving both the larger and smaller proteins that need to be detected in this assay.

First we needed to determine the purity of the subcellular fractions collected. This was done by loading WCL, cytosolic and organellar fractions from a single induced cell line onto a SDS-PAGE gel. The samples were loaded on the gel twice, separated by a prestained protein ladder that could be used as a visible marker to cut the membrane containing the transferred proteins into two blots. One could then be probed with a cytosolic marker using the rabbit polyclonal adenine phosphoribosyltransferase (APRT) antibody (1:1000 dilution). The other blot would be immunolabeled with the organellar control using the mouse monoclonal mitochondrial heat shock protein 70 (mtHSP70) antibody (1:1000 dilution). The secondary antibodies (1:2000 dilution) conjugated with HRP were either anti-rabbit (APRT) or anti-mouse (mtHSP70). The procedures of probing, washing and visualization were followed as described in 3.2.2.3.

If the subcellular fractions were mutually exclusive for one or the other antibodies, the samples were analysed again by western blot analysis to determine the subcellular localization of each of the α subunit variants. This time the primary antibody was the mouse monoclonal anti-V5 antibody (1:1000 dilution). The secondary antibody was again a goat anti-mouse antibody conjugated with HRP (1:2000 dilution).

3.3.4 PCR Verification of Positive Subunit Variant Cell

Since the tagged FL α subunit cell line can only be verified by detecting the mature C-terminal subunit peptide, we verified the positive cell lines used in the subcellular fractionation assay by PCR amplification of their gDNA. gDNA was isolated using the GenElute mammalian genomic DNA kit (Sigma-Aldrich) and the DNA concentrations were measured using the Thermo-Fisher Nanodrop spectrophotometer. Each of the α subunit variants was PCR amplified from 100 ng of gDNA using primers (Table 23) that annealed to the integrated plasmid DNA outside of the α subunit coding sequence (Table 24 and 25). Since each of the subunit variants produces an amplicon of significantly different size, the cell lines could be verified by resolving the PCR products on a 1% agarose gel. As a negative control, gDNA isolated from BF 427 wildtype parasites was used as a template for the same primer set.

Table 23 – Primers used the amplify the gDNA

	Forward Primer	Reverse Primer
Sequence	GTTACCCGTCCCTTATCAAC	GGAGTAATCTGATGGCACG

Table 24 – PCR reactions (50 µL)

Component	Concentration	FL α (µL)	N-Term (µL)	C-Term + 8 (µL)
MilliQ		32.87	32.6	32.5
10x Buffer without Mg^{2+}	1x	5	5	5
dNTPs (10 mM)	0.2 mM	1	1	1
Forward Primer (10 µM)	2 µM	1	1	1
Reverse primer (10 µM)	2 µM	1	1	1
Taq Polymerase	1 U	2.5	2.5	2.5
Mg^{2+}	2 mM	4	4	4
gDNA	100 ng	2.63	2.9	3

Table 25 – PCR program

Step	Temperature / °C	Time	Cycles
PCR activation	94	2 min	
Denaturation	94	30 s	34
Annealing	51	30 s	
Extension	72	2.5 min	
Final extension	72	7 min	

3.4 Immunofluorescence Assay

An immunofluorescence assay (IFA) was performed to visualize and further verify the localization of the α protein variants. Tetracycline induced cells were fixed and then permeabilized on a microscope slide. The heterologous α subunits were visualized by staining the cells with the V5 primary antibody and a secondary antibody conjugated with a fluorophore. Visualization was performed on a Zeiss fluorescent microscope connected to an Olympus DP73 CCD camera.

3.4.1 Cell Preparation

$2x10^7$ cells were harvested and thoroughly resuspended in 200 µL 1x PBS to prevent the cells from forming large aggregates before the fixative was added. Then 200 µL of 7.4% formaldehyde in 1x PBS (Table 26) was added and the solution was mixed. 40 µL of the fixed cells were applied to a cover slip and were incubated for 15 min at RT. Afterwards the buffer was removed and the cells were washed three times with 100 µL 1x PBS.

Table 26 – Fixing solution

Reagent	[Stock]	Amount for 2 mL	]Final]
PBS	1x	1.6 mL	1x
Formaldehyde	37%	0.4 mL	7.4%

The cells were then permeabilized for 10 min at RT with 100 µL of 0.1% Triton X-100 in 1x PBS. The cells were then washed three times with 1x PBS. Next the cells were blocked for 1 hour with 100 µL of 5.5% FBS in 1x PBS-T (Table 27). Then the cells were washed two times with 1x PBS.

Table 27 - Blocking Solution

Reagent	[Stock]	Amount for 2 mL	[Final]
PBS-T	1x	1.890 mL	1x
FBS	100%	110 µL	5.5%

While the controls were not done properly, two different primary antibodies (Table 28) were used to visualize either the tagged α subunit proteins (mouse V5 antibody, 1:200 dilution) in the induced cells or the mitochondrion itself (rabbit F_1-ATP synthase β subunit, 1:500 dilution) in the noninduced cells. 40 µL of the primary antibody solutions were incubated with the cells for 1 hour at RT. Then the cells were washed three times with 100 µL 1x PBS-T and two times with 100 µL 1x PBS. A goat anti-mouse secondary antibody conjugated with a Texas red fluor was diluted 1:400 (Table 29), while a goat anti-rabbit secondary antibody conjugated with the Alexa fluor 488 was also diluted 1:400. 40 µL of the secondary antibodies were added to the cells stained with the corresponding primary antibodies. The cells were then incubated at RT for 1 hour in the dark because the secondary antibodies are light sensitive. Again the

cells were washed as before, except this time they were covered to keep them shielded from the light.

Table 28 - Primary Antibody

Reagent	[Stock]	400 µL	[Final]
PBS-T	1x	280 µL	1x
BSA	10%	120 µL	3%
Antibody	-	2 µL	1:200

Table 29 - Secondary Antibody

Reagent	[Stock]	400 µL	[Final]
PBS-T	1x	280 µL	1x
BSA	10%	120 µL	3%
Antibody	-	1 µL	1:400

3.4.2 Viewing

The cover slips were mounted on microscope slides with Prolong Gold Antifade reagent containing DAPI (Invitrogen). The slides were stored laying down in the dark for 24 hours before taking pictures. Images were captured with a fluorescence microscope connected to an Olympus DP73 CCD camera. Different filters were used to visualize the secondary antibodies.

3.5 Blue Native PAGE

To determine if the V5 tagged FL α subunit was able to integrate into the F_oF_1 ATP-Synthase complex, a blue native PAGE (BN PAGE) was performed to analyse the assembled complex in its native form. For this purpose, mitochondria were hypotonically isolated from induced cells. Mitochondria from non-induced cells were also isolated and used as a negative control for the BN PAGE.

3.5.1 Mitochondria Purification

$5x10^8$ cells of both induced and non-induced cells were harvested by spinning at 1,300*g for 10 min at 4°C. Based on the number of cells harvested, the rest of the solutions required to complete the mitochondria isolation could be calculated. The cell pellet was resuspended in 20 mL SBG (Table 30) and spun again to wash the cells. Next the cells were resuspended in 2.6 mL of the hypotonic solution DTE (Table 31). The cell suspension was quickly transferred into a dounce, where 8 strokes from pestle B lysed the plasma membrane of the swollen cells. To restore isotonic conditions before the mitochondria became lysed, 0.6 mL of 60% sucrose was immediately added. This was followed with a differential centrifugation step performed at 15,000*g for 10 min at 4°C. The resulting pellet contained fragments of the plasma membrane and all the organelles. This pellet was then resuspended in 0.7 mL STM (Table 32), which resulted in a viscous solution due to released gDNA. This gDNA would interfere with the downstream applications, so 5.1 µL of both 1 M $MgCl_2$ and 0.1 M $CaCl_2$ were added to enhance the digestion conditions. Then 1.17 µL of 10 U/2.5 µL DNase was added and the solution was incubated on ice for 1 hour. Finally, 1.7 mL of STE (Table 33) was added to stop the DNA digestion. This crude mitochondrion purification was then centrifuged at 15,000*g for 10 min at 4°C. The supernatant was decanted and the mitochondria were flash freezed in liquid nitrogen before storing them at -80°C.

Table 30 – SBG (200 mL)

SBG	[Stock]	[Final]	200 mL
MilliQ			
NaCl		150mM	1.75g
Glucose		20mM	0.72g
NaH_2PO_4	0.2 M	20mM	1.4ml
Na_2HPO_4	0.2 M	20mM	18.6ml
Filled up with MilliQ to:			200ml

Table 31 – DTE (100 mL)

DTE	[Stock]	[Final]	100 mL
MilliQ			90 mL
Tris (pH 8.0)	1 M	1mM	100 µL
EDTA (pH 8.0)	0.5 M	1mM	200 µL
Filled up with MilliQ to:			100 mL

Table 32 – STM (100 mL)

STM	[Stock]	[Final]	100 mL
MilliQ			75 mL
Sucrose		250 mM	8.56 g
Tris (pH 8.0)	1 M	20 mM	2 mL
$MgCl_2$	1 M	2 mM	200 µL
Filled up with MilliQ to:			100 mL

Table 33 – STE (100 mL)

1xSTE	[Stock]	[Final]	100 mL
MilliQ			75 mL
Sucrose		250 mM	8.56 g
1M Tris (pH 8.0)	1 M	20 mM	2 mL
0.5M EDTA (pH 8.0)	0.5 M	2 mM	200 µL
Filled up with MilliQ to:			100 mL

3.5.2 BN PAGE

The isolated mitochondria were then lyzed in 40 µL of 1 M aminocaproic acid and a final concentration of 2.5% dodecyl maltoside. The protein concentration of the lyzed mitochondria was determined by performing a Bradford assay. The F_oF_1-ATP synthase can be easily visualized by BN PAGE when 4 µg of mitochondrial proteins are prepared with 1.5 µL of loading dye and the final volume is brought to 20 µL by adding additional 1M aminocaproic

acid. The solution was incubated on ice for 10 min before it is loaded on a pre-cast 3-12% Bis-Tris gradient NativePAGE Novex gel (Invitrogen). After assembling the gel into the mini tank apparatus, 200 mL of cathode buffer (Table 34) were added to the front chamber, while anode buffer (Table 34) was added behind the gel until the chamber was half full. 10 µL of the nativeMark unstained protein standard was also loaded. After loading the induced and non-induced mitochondria samples, the BN PAGE was run for around 3 hours at 150 V at 4°C. Finally, the resolved protein complexes were transferred to a membrane under normal conditions. The resulting western blot analysis was then performed as stated previously, using the F_1-ATP synthase β subunit antibody or the monoclonal V5 antibody.

Table 34 – Cathode and anode buffer

Reagent	**10x Cathode Buffer**			**10x Anode Buffer**		
	[Stock]	**100 mL**	**[Final]**	**[Stock]**	**100 mL**	**[Final]**
Bis Tris (pH 7.0)	1 M	15 mL	150 mM	1 M	15 mL	150 mM
Tricine	1 M	50 mL	500 mM			
Coomassie Brilliant Blue G250	20%	100 µL	0.02%			
Filled up with MilliQ to:		100 mL			100 mL	

4. Results

4.1 Plasmid Used for the Overexpression of 3V5 Tagged α Fragments

To discern if the cleaved octapeptide is capable of acting as a mNTS for the mature C-terminal α subunit, we needed to clone various α subunit fragments into the *T. brucei* overexpression plasmid, pT7-3V5-PAC. First, the circular plasmid needs to be linearized with restriction enzymes that will produce sticky ends that are complementary to the digested PCR amplicons. The pT7-3V5-PAC plasmid was digested with BamHI and HindIII and resolved on a 1% agarose gel containing ethidium bromide. The expected linearized plasmid (5909 nucleotides (nt)) was observed (Figure 11) and subsequently gel extracted for downstream cloning events.

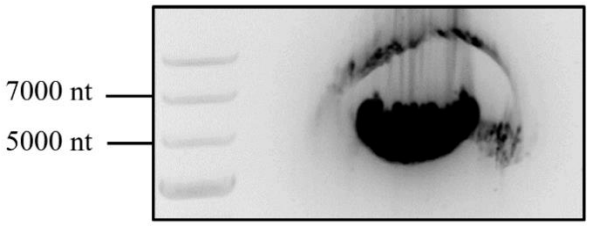

Figure 11 – Agarose gel showing the digested plasmid pT7-3V5-PAC observed at the expected size of 5909 nt next to a 1kb Plus DNA ladder

4.2 PCR Amplification of the Various α Gene Fragments

To obtain the three different fragments of the α subunit gene to clone into the pT7-3V5-PAC plasmid, PCR amplification was performed with the primer pairs described previously. To ensure we generated enough DNA to insert into the backbone vector, two PCR reactions were performed for each gene fragment. The synthesized DNA was subsequently resolved on a 1% agarose gel containing ethidium bromide to separate the amplicons of expected size (FL α – 1752 nt, N-term - 453 nt, C-term + 8 - 1296 nt) from any possible misprimed products (Figure 12). While some additional bands were observed at the chosen annealing temperature of 53°C, the predominate band of the expected size was gel extracted and used for subsequent cloning steps.

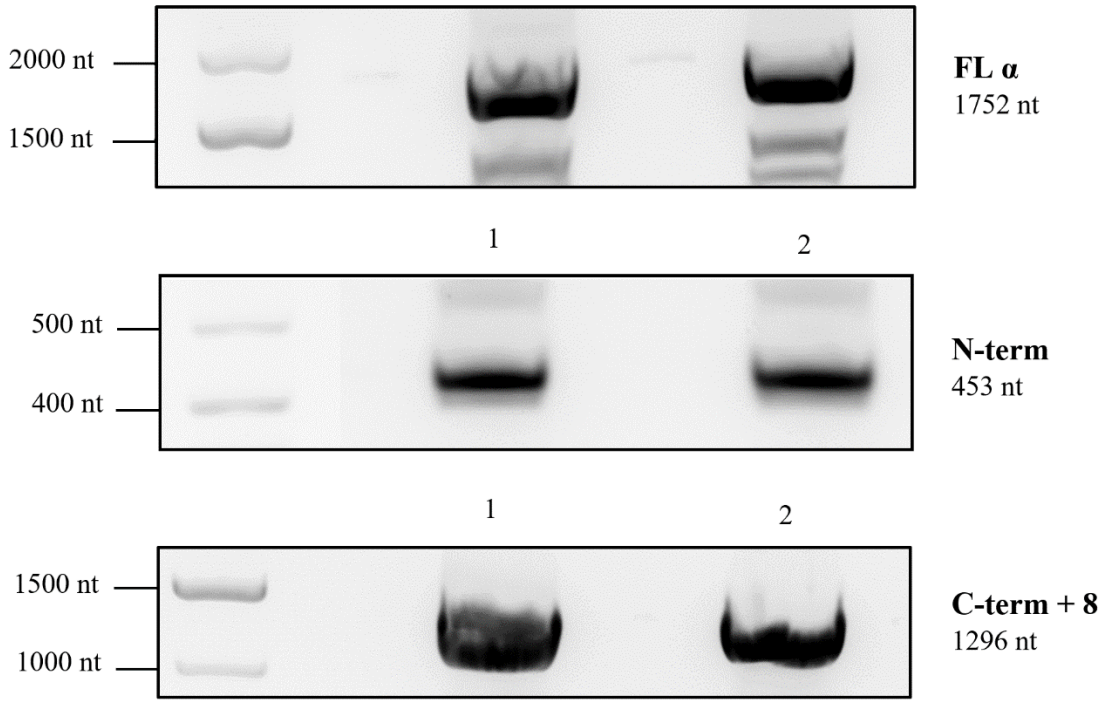

Figure 12 – PCR products of each FL α, N-term and C-term + 8 were resolved on an agarose gel. Two PCR reactions (1, 2) were performed for each fragment. The sizes of the DNA ladder are marked on the left, the expected sizes of each fragment are mentioned on the right of the picture

4.3 Creation and Confirmation of Proper Plasmid Construction

The gel extracted amplicons were also digested with BamHI and HindIII and then cleaned up to remove undesired components for downstream cloning events. The digested amplicons were then ligated with the linearized plasmid in a 3:1 insert: vector molar ratio. The ligations were then used to transform chemically competent cells. Around 100 colonies per transformation arose on an agar plate and plasmid DNA was isolated from four colonies from each transformation. 1 µg of DNA was digested with BamHI and HindIII before being analyzed on a 1% agarose gel containing ethidium bromide. Positive clones should produce two bands, one for the plasmid (5909 nt) and one for the insert (FL α - 1752 nt, N-term - 453 nt, C-term + 8 - 1296 nt). Figures 13, 14 and 15 indicate that all four clones of FL α and N-term were positive. Similar success was observed for three out of four C-terminal + 8 as one digestion reaction was lost due to spillage.

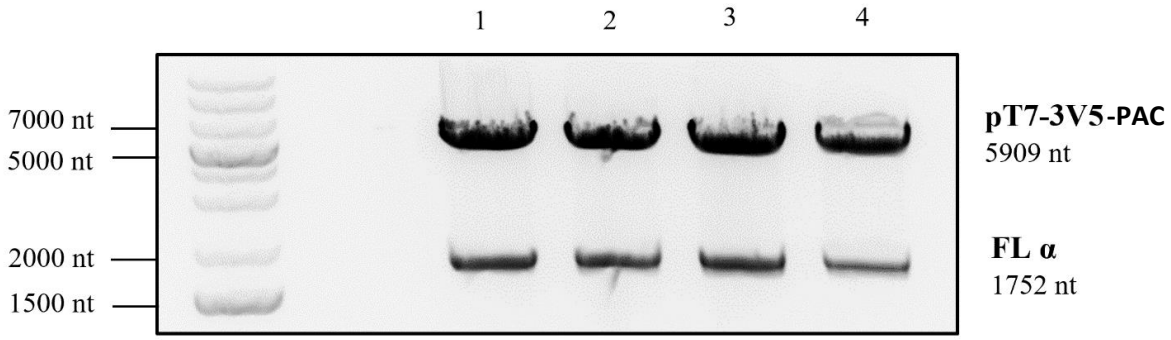

Figure 13 – BamHI and HindIII restriction digest results of four FL α clones (1, 2, 3, 4). Each of the lanes show the expected plasmid at 5909 nt and the FL α insert of 1752 nt.

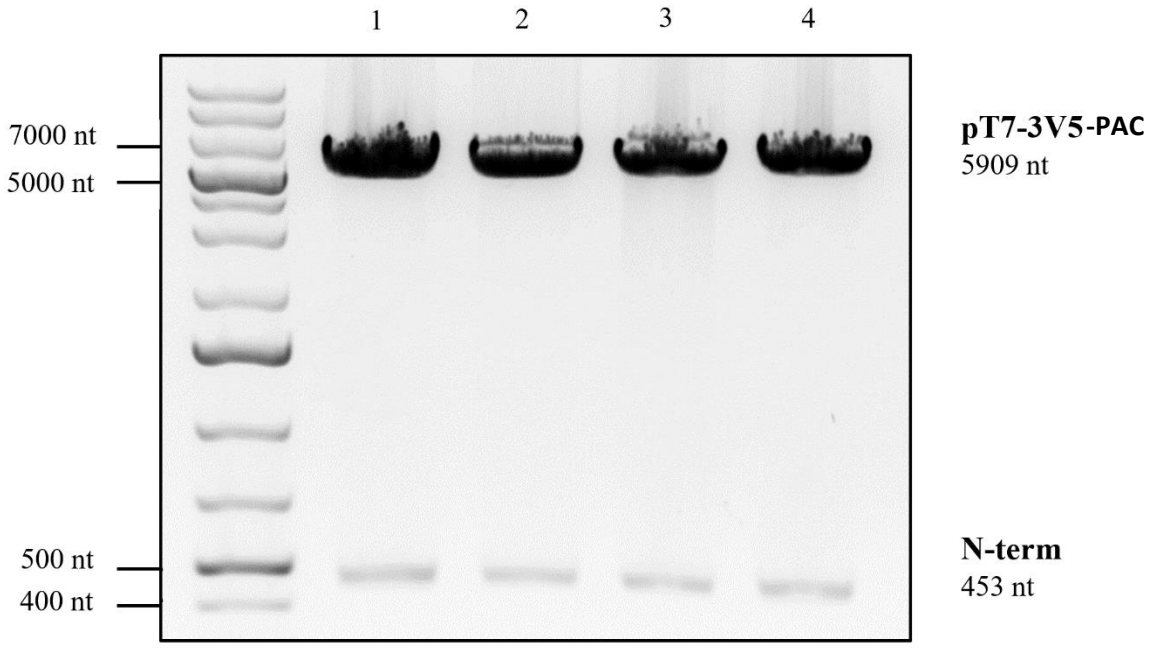

Figure 14 – BamHI and HindIII restriction digest results of four N-term clones (1, 2, 3, 4). Each of the lanes show the expected plasmid at 5909 nt and the N-term insert of 453 nt.

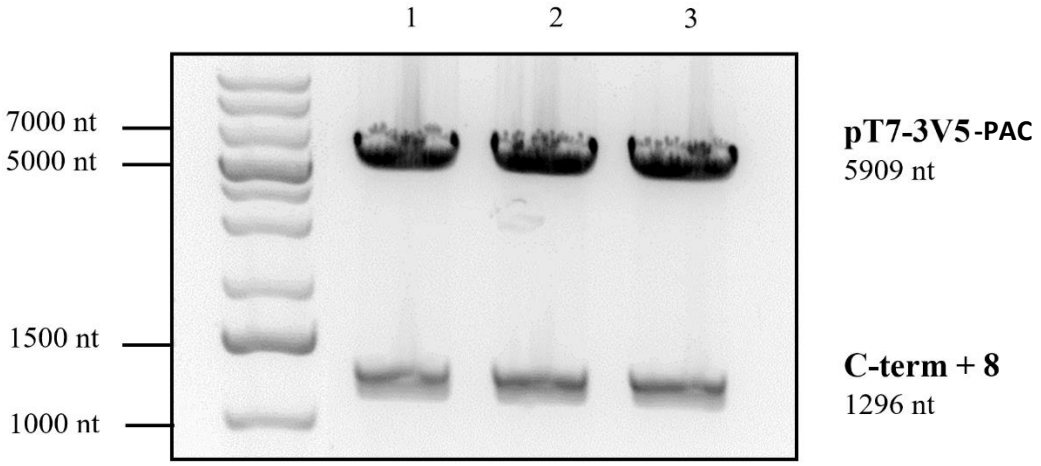

Figure 15 - BamHI and HindIII restriction digest results of three C-term + 8 clones (1, 2, 3). Each of the lanes show the expected plasmid at 5909 nt and the C-term + 8 insert of 1296 nt

Finally, one of each of the positive α fragment plasmids that produced the expected digested fragments was sent for sequencing to make sure that no errors were introduced into the coding sequence during the cloning events. The sequencing results contained chromatograms of good quality and they only indicated a few silent mutations (Table 35, Figure 16 and 17). These results further verified the success of the cloning.

Table 35 – Summary of sequencing results

Insert	Nucleotide Position	Nucleotide Change	Codon	Amino Acid Change	Sequencing Direction
FL α	240	T/C	ATT/ATC	No change	forward
	519	C/T	ATC/ATT	No change	forward
	1398	A/G	CAA/CAG	No change	reverse
N-Term	240	T/C	ATT/ATC	No change	forward & reverse
C-term + 8	519	C/T	ATC/ATT	No change	forward

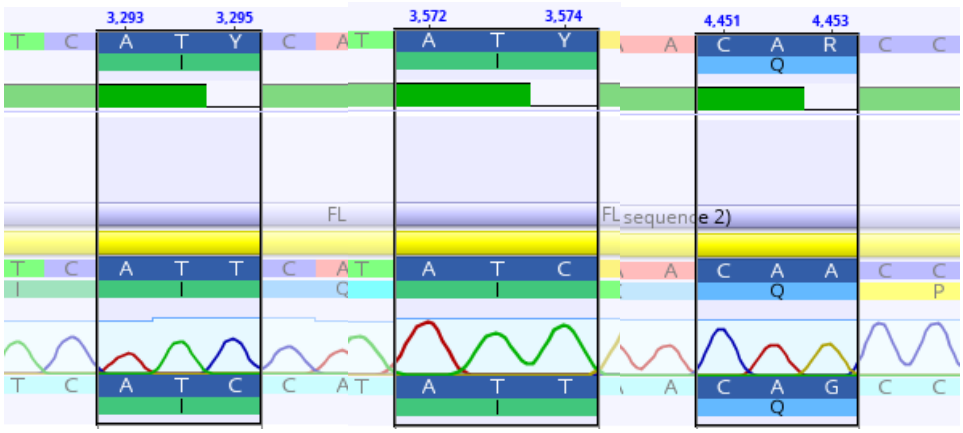

Figure 16 – Mutations observed in the chromatogram of FL α subunit, which did not lead to any amino acid change.

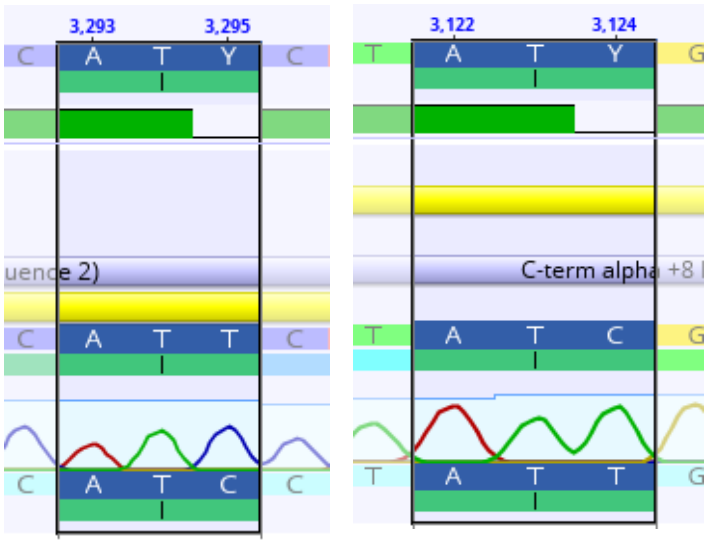

Figure 17 – Mutation observed in the chromatogram of N-term (left) and C-term + 8 (right), which did not lead to any amino acid change.

4.4 Western Blot Analysis of Transfected Cell Lines

After the positive selection of transfected *T. brucei* 29.13 cell lines, western blot analysis was performed to verify that the resulting clones express the appropriate V5 tagged alpha variant. Whole cell lysates (WCL) were prepared from both tetracycline-induced (+) and non-induced (-) cells. These samples were resolved on polyacrylamide gel and transferred to a polyvinyl membrane that was then probed with the V5 antibody to determine the amount of protein expression for each of the heterologous proteins (Figures 18, 19 and 20). While there

is some leaky expression of the tagged α subunit products in the uninduced samples, these levels are drastically increased in the tetracycline induced samples. The expected size of FL α is smaller than it would be for the full protein as only the mature C-term still attached to the V5 tag can be detected. Due to the rapid first α cleavage after protein expression, no FL α still consisting of both its N-term and C-term + 8 can be detected.

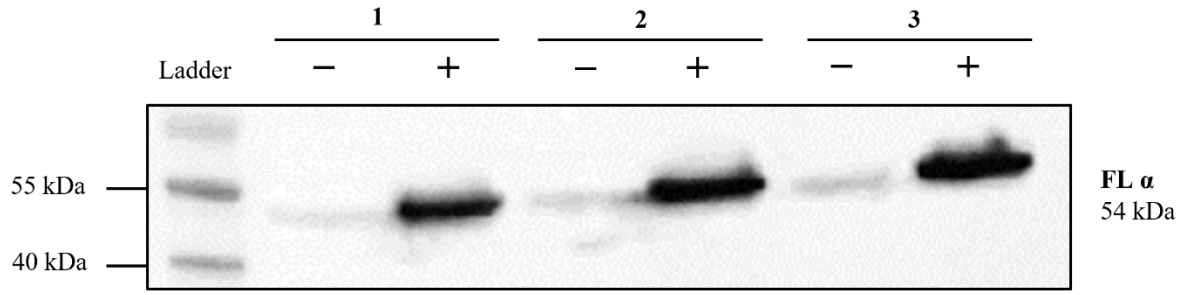

Figure 18– Protein expression and size verification of three FL α clones (1, 2, 3), non-induced (-) and induced for two days (+) with 1 mg/mL tetracycline.

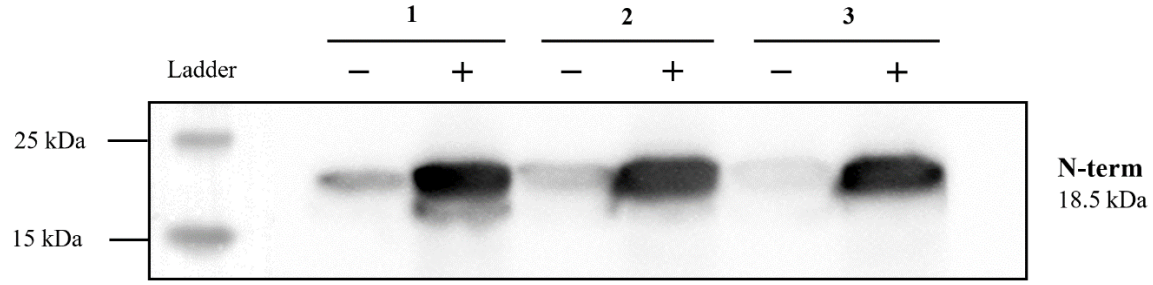

Figure 19 – Protein expression and size verification of three N-term clones (1, 2, 3), non-induced (-) and induced for two days (+) with 1 mg/mL tetracycline.

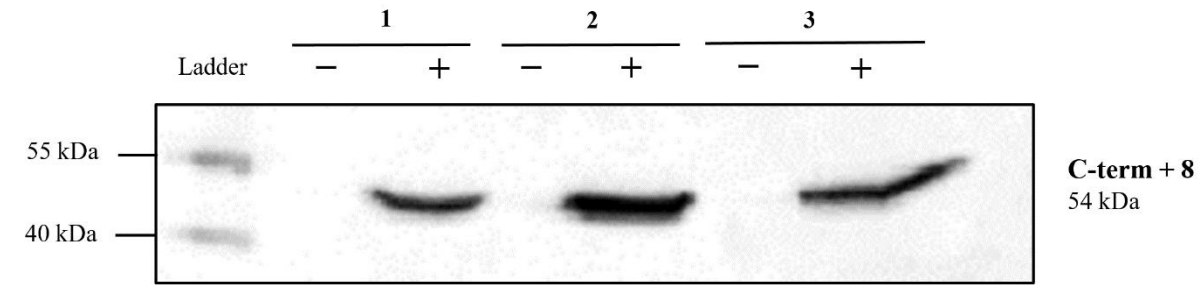

Figure 20 – Protein expression and size verification of three C-Term + 8 clones (1, 2, 3), tetracycline non-induced (-) and induced for two days (+) with 1 mg/mL tetracycline

4.5 Subcellular Localization of the α Subunit Variants

The three α subunit variant *T. brucei* cell lines capable of tetracycline inducible expression were treated with digitonin to create a soluble cytosolic fraction and an insoluble organellar fraction. These samples were then analyzed by Western blots performed with different primary antibodies that acted as controls for the proper segregation of these subcellular fractions. As illustrated in Figure 21, the mt marker mtHSP70 was only detected in the organellar fraction, whereas the cytosolic marker APRT was observed in just the cytosolic fractions. This indicates that the digitonin treated cells were all lysed since no cytosolic marker was detected in the organellar fraction. Since there is no cross-contamination between the cytosolic and organellar fractions, we probed the same samples with a V5 antibody to determine where the tagged α subunit variants were targeted within the cell (Figure 22). No signal was detected in the cytosolic fractions of any of the α subunit variant cell lines. This result was expected for the FL and N-terminal α subunits, both of which contain a known mNTS. Since the C-terminal + 8 was also detected in just the organellar fraction, it suggests that the α octapeptide that is eventually cleaved from the mature C-terminal α subunit can act as a targeting signal if the first octapeptide cleavage (L151) occurs in the cytosol. Additional controls would have to be performed to rule out the possibility that there is an additional mt targeting sequence that resides outside of the octapeptide.

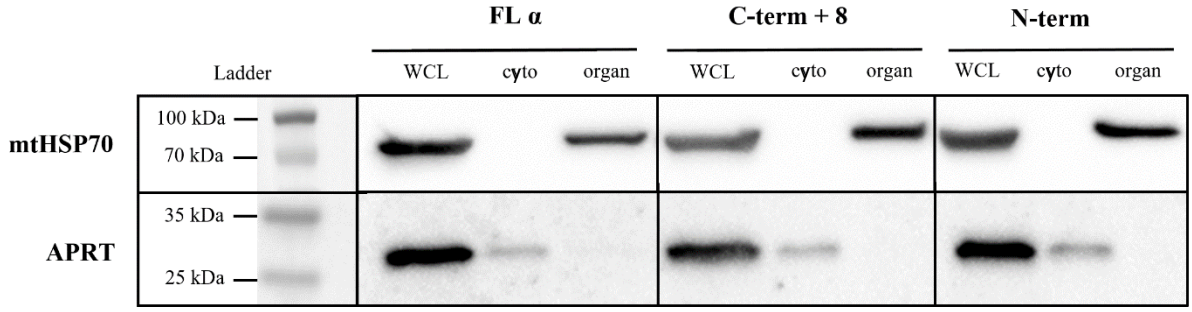

Figure 21 – Western blot analysis to analyze the efficiency of the digitonin subcellular fraction. Antibodies diluted 1:1000 against the cytosolic marker APRT (26 kDa) and the mtHSP70 (70 kDa) were used to probe blots containing whole cell lysates (WCL), as well as the cytosolic (cyto) and organellar (organ) fractions.

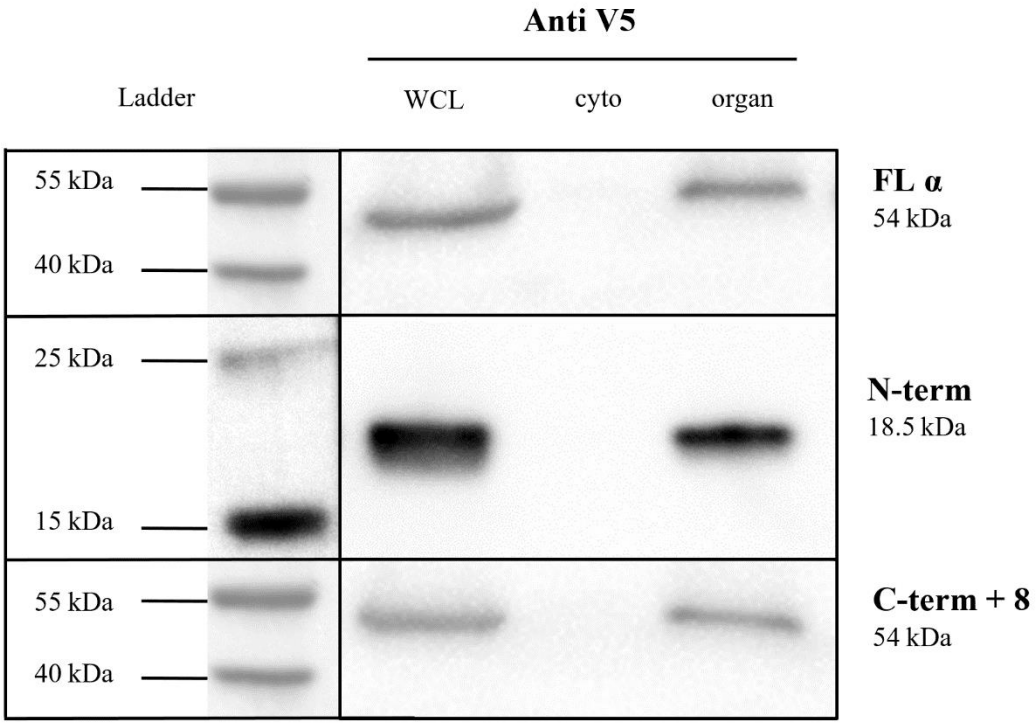

Figure 22 – Western blot analysis to examine the subcellular localization of the V5 tagged α subunit variants. A V5 antibody diluted 1:2000 was used to probe blots containing whole cell lysates (WCL), cytosolic (cyto) and organellar (organ) fractions of each α variant cell line. The expected sizes for each heterologous α subunit protein are listed on the right.

4.6 Verification of the Heterologous α Subunit Variants Expressed by the Analyzed *T. brucei* Cell Lines

Since we are not able to distinguish between the protein products derived from the integration of the ectopic FL and C-terminal α subunits on western blots, we wanted to verify that the proteins expressed in each cell line were indeed being synthesized from the expected DNA sequence. Therefore, genomic DNA (gDNA) was harvested from each of the transfected cell lines. PCR was then performed to amplify the DNA sequence of the integrated α subunit variants with primers that would anneal to regions of the backbone vector that lay just outside of the α subunit coding region. The gDNA from BF 427 wildtype cells were isolated as used as a negative control. The PCR reactions were then resolved on a 1% agarose gel (Figure 23). Each cell line generated an amplicon of the expected size, confirming that all three α subunit variants were correctly represented.

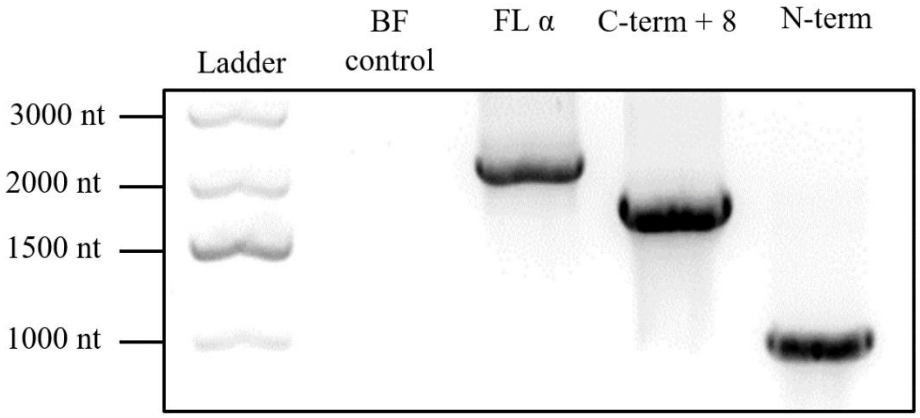

Figure 23 – PCR products amplified from the isolated gDNA of BF 427 wildtype cells and PF 29.13 cells lines expressing each of the α subunit variants.

4.7 Verification of the Subcellular Localization of the α Subunit Variants by Immunofluorescent Microscopy

Since the crude subcellular fractionation assay with digitonin is only able to separate the cytosol from all of the remaining organelles, it is important to verify that the α subunit variants were indeed specifically targeted to the mitochondrion and not some other *T. brucei* organelle. Therefore, we visualized the localization of the tagged α subunit in each of the cell lines using immunofluorescence assays with the V5 antibody (Figure 24). While proper controls to define the localization of the *T. brucei* mitochondrion in each V5 image, the uninduced FL α subunit cell line was analyzed with an antibody to F_oF_1-ATP synthase β subunit that defines the mitochondrion. The subcellular pattern visualized in the V5 images for each of α subunit variants clearly resembles the mitochondrion observed with the anti-β subunit antibody. Importantly, none of the cell lines displayed a signal that would represent the cytosol of the parasite. These results verify that the organellar localization previously detected in the digitonin subcellular fractions was due to the mt targeting of the α subunit variants.

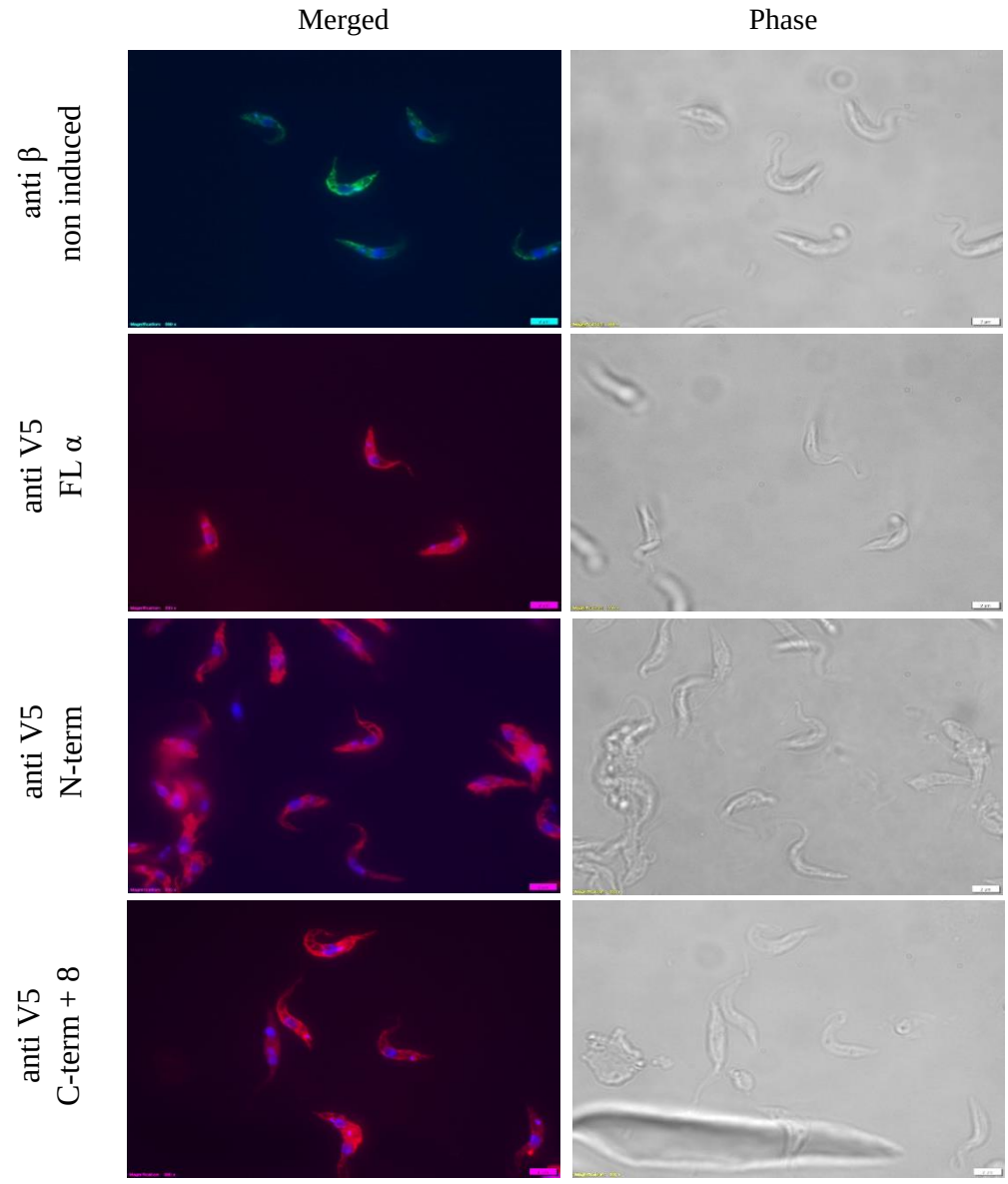

Figure 24 – Images obtained from an immunofluorescence analysis. The left column displays merged images of the parasites incubated with various antibodies (red signal) and stained with DAPI to indicate the nuclear and mt DNA (blue dots). The right column presents phase contrast images obtained from the same PF *T. brucei* cells.

4.8 The Tagged FL α Subunit is Incorporated into the ATP Synthase

To further analyze the localization of the heterologous α subunit variants, we analyzed whether the resulting tagged C-terminal α subunit from the expressed FL α subunit is able to get incoporated into the FoF_1-ATP synthase. Isolated mitochondria from tetracycline induced and non-induced FL α subunit cells were resolved on a native polyacrylamide gel and then transferred onto a PVDF membrane. As a positive control, one blot was probed with the F_oF_1-

ATP synthase β subunit antibody (Figure 25). This produced all three expected bands representing the F_1-ATP synthase and the monomers and dimers of the F_oF_1-ATP synthase complex. When probed with the V5 antibody, a similar pattern was detected in the tetracycline induced cell lines. This indicates the successful incorporation of at least the V5-tagged C-terminal α subunit into the complex.

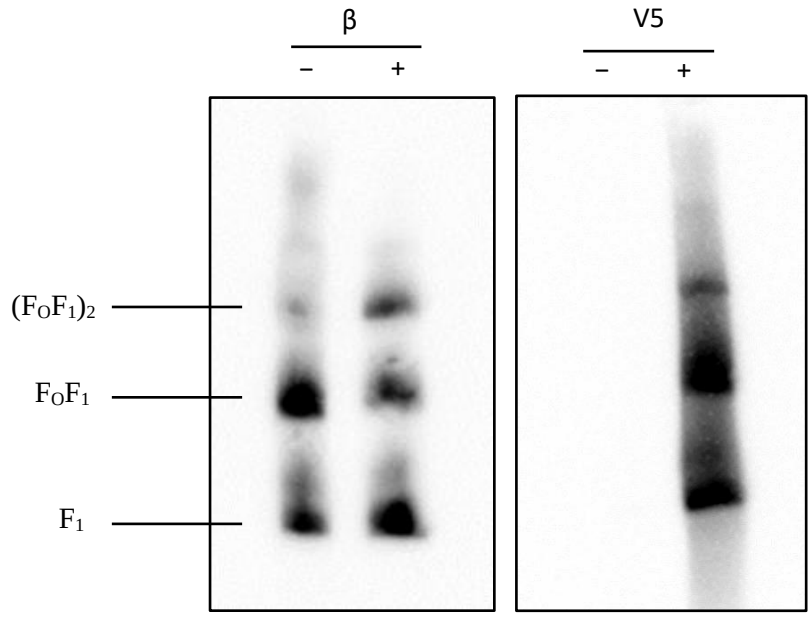

Figure 25 – BN gels resolving mitochondria isolated from either non-induced (-) or induced for two days (+) FL α subunit cells. The blots were probed with the F_1-ATP synthase β subunit antibody (left blot) or the anti-V5 antibody (right blot). The various isoforms of the ATP synthase are labeled on the left.

5. Discussion

The *T.brucei* ATP synthase α subunit has a unique internal octapeptide that is proteolytically cleaved from the mature protein. This results in a functional complex consisting of a distinct N-terminal and C-terminal α peptide (Montgomery et al., 2018; Gahura et al., 2018). Since the ATPase enzyme is essential in the infectious form of the parasite (Šubrtová et al., 2015; Schnaufer et al., 2005), we would like to determine if this cleavage is required for the proper function of the enzyme. The clearest evidence to demonstrate the necessity of this cleavage would be to deplete the responsible protease(s) and see if it affects the BF F_oF_1-ATPase activity. To narrow the potential list of protease candidates, other experiments in the lab are simultaneously being performed to determine where the cleavage(s) occurs in the parasite. While it would not be surprising if both of the internal α cleavage events occur within the mitochondrion, we noticed an interesting result if you presume that the first proteolytic cleavage (L151) occurs in the cytosol. When the protein sequence of the α C-terminal protein containing the octapeptide (152-584 α residues) is analyzed by the MitoProt application, it predicts (0.83 probability) that the octapeptide is the beginning of a 14 residue mNTS (MVTRSRRLLDSTLGK). Therefore, we explored if this signal could target an already cleaved C-terminal α subunit into the mitochondria. If yes, this might suggest that the first of the two α subunit proteolytic events actually occurs in the cytosol of the parasite.

To verify whether the cleaved octapeptide can indeed act as a mNTS for the C-terminal α subunit within the parasite, we created a series of inducible protein expression plasmids containing FL (1-584), N-terminal (1-151) or a C-terminal α subunit retaining the octapeptide (151-584). The localization of these proteins fused with a C-terminal V5 tag were analyzed in cells that had been gently lysed with 0.015% digitonin to obtain a cytosolic and an organellar fraction by differential centrifugation (Schneider et al., 2007). Probing our fractionated samples with control antibodies indicated that we successfully separated the mitochondrion from the cytosol. The western blot analyses of these fractions isolated from all three α subunit cell lines demonstrated that each α variant was predominantly targeted to the mitochondria. This was further verified by the mitochondrial staining observed in these cell lines when analyzed by immunofluorescence microscopy. Finally, we determined that the V5 tagged version of the FL α subunit is successfully incorporated into an assembled F_OF_1-ATP synthase complex by western blot analysis of isolated mitochondria resolved on blue-native gels. These preliminary

data suggest that if the first cleavage of the α octapeptide occurred in the cytosol, the C-terminal α subunit could still be properly imported into the mitochondrion.

The mitochondrial localization of the C-term α subunit still attached to the octapeptide can be interpreted in two ways. One is that the octapeptide is sufficient to target the C-terminal α subunit to the mitochondria. The other is that the C-terminal α subunit has a second intrinsic targeting sequence within this portion of the protein. To test these hypotheses, we can fuse the sequence of the cleaved α subunit octapeptide to a non-mitochondrial protein like mNeon green (mNG). As mNG is a protein that does not contain a mNTS, detection of the mNG + α subunit octapeptide in the organellar fraction of the cell would suggest that the octapeptide is sufficient as a mt targeting signal. However, to be completely certain that the overexpression of just mNG does not lead to mt targeting, the subcellular localization of mNG expression from the pT7-3V5-PAC vector should be determined. In addition, it would be helpful to generate a pT7-3V5-PAC vector that expresses the mature C-terminal α subunit. If this α subunit variant is not targeted to the mitochondrion, it would further verify that mt targeting sequence is limited to the octapeptide. Conversely, if this control is localized within the mitochondrion, then it would suggest that the mNTS of the C-terminal α subunit is larger than the octapeptide or there is a mt targeting sequence that resides somewhere downstream. As previously mentioned, such an internal mt targeting sequence has already been demonstrated for the *T. brucei* alternative oxidase (Hamilton et al., 2014).

The immunofluorescence assay (IFA) images obtained for the FL, N-terminal and C-terminal + 8 α subunit cell lines illustrate the prototypical staining of the PF *T. brucei* mitochondrion. This is further verified when these images are compared to uninduced cells immunolabeled with an anti-ATP synthase β subunit antibody. Unfortunately, our IFA results lack a proper control that would verify the localization of the mitochondrion within the same cell that was examined for the expression of the α subunit variants. There are two different ways to properly perform this experiment when time permits. One method is to use a mitochondrial stain such as tetramethylrhodamine, ethyl ester (TMRE). TMRE is a positively charged red-orange fluorescent stain that accumulates easily in the mitochondria due to its membrane potential. Alternatively, it is possible to use antibodies specific to mitochondrial proteins. To be able to distinguish the fluorescence of the mt control protein and the tagged α

subunit variants, it is necessary to use primary antibodies produced in different animals that can be detected by secondary antibodies conjugated with two different colored fluorophores (i.e. FITC and Texas RED). Since the commercially available V5 antibody used for these experiments is a monoclonal antibody produced in mice, we could have chosen any one of the rabbit antibodies produced in the lab to various subunits of the mt ATP synthase. Then it would be possible to obtain two images of the same parasite using two different filters on the fluorescent microscope. These images could then be overlapped to show their mutual subcellular localization.

We were successfully able to demonstrate that the overexpressed tagged α subunit variants were localized to the mitochondrion by a crude subcellular assay and by IFA. To further examine if these heterologous proteins were being properly targeted, we probed western blots of BN PAGE gels with the V5 antibody. Indeed, we demonstrated that the tagged FL α subunit gets incorporated into the assembled F_1-ATP synthase and F_oF_1-ATP synthase monomers and dimers. This signal was not detected in the resolved mitochondria isolated from the uninduced FL α subunit parasites and it produced a pattern similar to that observed when the same material was probed with the antibody raised against the F_1-ATP synthase β subunit. However, no conclusion can be made about whether the enzymatic complex is functionally active when it contains a V5 tagged α subunit. Unpublished data from the lab suggests that a heterologous V5 tagged α subunit is not able to rescue the growth phenotype of an RNAi α subunit cell line. However, the results of this experiment are not yet conclusive as this complementation experiment is complicated and the negative result might be due to other variables besides enzymatic functionality.

Two different experimental methods could be employed to determine if the F_oF_1-ATP synthase complex containing a V5 tagged α subunit is enzymatically active. The first assay utilizes the ATP Bioluminescence Assay Kit HS II (Roche) to measure the concentration of ATP produced from isolated mitochondria when they are provided the appropriate substrates. The principal of this assay relies on the ATP dependency of the supplied luciferase to oxidize the substrate luciferin and create light that can be quantified. Since we want to measure the amount of ATP produced from F_oF_1-ATP synthase coupled with an active ETC, it is essential that intact and charged mitochondria are isolated for this assay (Zíková et al., 2009). Therefore, a crude mt preparation is created using 0.015% digitonin. ATP production is then activated by the addition of oxidative phosphorylation substrates ADP and succinate. Since mt substrate phosphorylation reactions can also contribute to the ATP pool (Bochud-Allemann et al., 2002),

specific inhibitors to succinate dehydrogenase (malonate) and the ADP/ATP carrier (atractyloside) are added to determine the proportion of ATP produced by F_oF_1-ATP synthase (Schneider et al., 2007).

Since the F_oF_1-ATP synthase can also rotate in reverse, Sumner reagent can be utilized in an assay to detect the release of free phosphate when ATP is hydrolyzed (Law et al., 1995). Briefly, mitochondrial pellets are resuspended in an assay buffer and the addition of ATP starts the reaction. To stop the ATPase activity, 70% perchloric acid is added to precipitate all of the proteins. The samples are then spun down and Sumner reagent is added to the supernatant. The absorbance at 610 nm is recorded for each enzymatic reaction and compared to a free phosphate standard curve. Therefore, these two activity based assays can be performed to provide insight into the functionality of the ATP synthase complex comprised of a V5 tagged α subunit.

6. References

Allen, J.W., Feruguson, S.J. & Ginger, M.L. Distinctive biochemistry in the trypanosome mitochondrial intermembrane space suggests a model for stepwise evolution of the MIA pathway for import of cysteine-rich proteins. FEBS Letters 582, 2817-2825 (2008)

Babokhov, P., Sanyaolu, A.O., Oyibo, W.A., Fagbenro-Beyioku, A.F. & Iriemenam, N.C. A current analysis of chemotherapy strategies for the treatment of human African trypanosomiasis. Pathogens and Global Health 107(5), 242-252 (2013)

Basu S., Leonard J.C., Desai N., Mavridou D.A., Tang K.H., Goddard A.D., Ginger M.L., Lukeš J. & Allen J.W. Divergence of Erv1-associated mitochondrial import and export pathways in trypanosomes and anaerobic protists. Eukaryotic Cell 12(2), 343-355 (2013)

Blattner J., Helfert S., Michels P. & Christine Clayton. Compartmentation of phosphoglycerate kinase in *Trypanosoma brucei* plays a critical role in parasite energy metabolism. Proceedings of the National Academy of Sciences of the United States of America 95(20), 11596-11600 (1998)

Bochud-Allemann N. & Schneider A. Mitochondrial substrate level phosphorylation is essential for growth of procyclic Trypanosoma brucei. The Journal of Biological Chemistry 277(36), 32849-32854 (2002)

Büscher P., Cecchi G., Jamonneau V. & Priotto G. Human African trypanosomiasis. Lancet 390(10110), 2397-2409 (2017)

Carroll J., Fearnley I.M., Skehel J.M., Runswick M.J., Shannon R..J., Hirst J. & Walker J.E. The post-translational modifications of the nuclear encoded subunits of complex I from bovine heart mitochondria. Molecular and Cellular Proteomics 4(5), 693-699 (2005)

Chaudhuri M., Ott R.D. & Hill G.C. Trypanosome alternative oxidase: from molecule to function. Trends in Parasitology 22(10), 484-491 (2006)

Desy S., Mani J., Harsman A., Käser S. & Schneider A. TbLOK1/ATOM19 is a novel subunit of the noncanonical mitochondrial outer membrane protein translocase of Trypanosoma brucei. Molecular Microbiology 102(3), 520-529 (2016)

Dimroth P., Kaim G. & Matthey U. Crucial role of the membrane potential for ATP synthesis by F(1)F(o) ATP synthases. The Journal of Experimental Biology 203, 51-59

Eckers E., Cyrklaff M., Simpson L. & Deponte M. Mitochondrial protein import pathways are functionally conserved among eukaryotes despite compositional diversity of the import machineries. Biological Chemistry 393(6), 513-524 (2012)

Eckers E., Petrungaro C., Gross D., Riemer J., Hell K. & Deponte M. Divergent molecular evolution of the mitochondrial sulfhydryl:cytochrome C oxidoreductase Erv in opisthokonts and parasitic protists. The Journal of Biological Chemistry 288(4), 2676-2688 (2013)

Gahura O., Šubrtová K., Váchová H., Panicucci B., Fearnley I.M., Harbour M.E., Walker J.E. & Zíková A. The F_1 -ATPase from Trypanosoma brucei is elaborated by three copies of an additional p18-subunit, The FEBS Journal 285(3), 614-628 (2018)

Garg S., Stölting J., Zimorski V., Rada P., Tachezy J., Martin W.F. & Gould S.B. Conservation of Transit Peptide-Independent Protein Import into the Mitochondrial and Hydrogenosomal Matrix. Genome Biology and Evolution 7(9), 2716-2726 (2015)

Gentle I.E., Perry A.J., Alcock F.H., Likić V.A., Dolezal P., Ng E.T., Purcell A.W., McConnville M., Naderer T., Chanez A.L., Charrière F., Aschinger C., Schneider A., Tokatlidis K. & Lithgow T. Conserved motifs reveal details of ancestry and structure in the small TIM chaperones of the mitochondrial intermembrane space. Molecular Biology and Evolution 24(5), 1149-1160 (2007)

Gualdrón-López M., Brennand A., Hannaert V., Quiñones W,. Cáceres A.J., Bringaud F., Concepción J.L. & Michels P.A.. When, how and why glycolysis became compartmentalised in the Kinetoplastea. A new look at an ancient organelle. International Journal for Parasitology 42(1), 1-20 (2012)

Hamilton V., Singha U.K., Smith J.T., Weems E. & Chaudhuri M. Trypanosome alternative oxidase possesses both an N-terminal and internal mitochondrial targeting signal. Eukaryotic Cell 13(4), 539-547 (2014)

Harsman A. & Schneider A. Mitochondrial protein import in trypanosomes: Expect the unexpected. Traffic 18(2), 96-109 (2016)

Jamonneau V., Ilboudo H., Kaboré J., Kaba D., Koffi M., Solano P., Garcia A., Courtin D., Laveissière C., Lingue K., Büscher P. & Bucheton B. Untreated human infections by

Trypanosoma brucei gambiense are not 100% fatal. PLOS Neglected Tropical Diseases 6(6), e1691 (2012)

Kaufer A., Ellis J., Stark D. & Barratt J. The evolution of trypanosomatid taxonomy. Parasites & Vectors 10(1), 287 (2017)

Klusch N., Murphy B.J., Mills D.J., Yildiz Ö. & Kühlbrandt W. Structural basis of proton translocation and force generation in mitochondrial ATP synthase. eLife 6, e33274 (2017)

Kolev N.G., Ramey-Butler K., Cross G.A., Ullu E. & Tschudi C. Developmental progression to infectivity in Trypanosoma brucei triggered by an RNA-binding protein. Science 338(6112), 1352-1353

Law R.H., Manon S., Devenish R.J. & Nagley P. ATP synthase from Saccharomyces cerevisiae. Methods in Enzymology 260, 133–163 (1995)

Mach J., Poliak P., Matusková A., Zárský V., Janata J., Lukeš J. & Tachezy J. An Advanced System of the Mitochondrial Processing Peptidase and Core Protein Family in Trypanosoma brucei and Multiple Origins of the Core I Subunit in Eukaryotes. Genome Biology and Evolution 5(5), 860-875 (2013)

Mani J., Desy S., Niemann M., Chanfon A., Oeljeklaus S., Pusnik M., Schmidt O., Gerbeth C., Meisinger C., Warscheid B. & Schneider A. Novel mitochondrial protein import receptors in Kinetoplastids reveal convergent evolution over large phylogenetic distances. Nature Communications. 6, 6646 (2015).

Mani J., Meisinger C. & Schneider A. Peeping at TOMs-Diverse Entry Gates to Mitochondria Provide Insights into the Evolution of Eukaryotes. Molecular Biology and Evolution. 33, 337–351 (2016).

Matthews K.R. 25 years of African trypanosome research: From description to molecular dissection and new drug discovery. Molecular and Biochemical Parasitology 200(1-2), 30-40

Mazet M., Morand P., Biran M., Bouyssou G., Courtois P., Daulouède S., Millerioux Y., Franconi J.M., Vincendeau P., Moreau P. & Bringaud F. Revisiting the central metabolism of the bloodstream forms of Trypanosoma brucei: production of acetate in

the mitochondrion is essential for parasite viability. PLOS Neglected Tropical Diseases 7(12), e2587

Montgomery M.G., Gahura O., Leslie A.G.W., Zíková A. & Walker JE. ATP synthase from Trypanosoma brucei has an elaborated canonical F_1-domain and conventional catalytic sites. Proceedings of the National Academy of Sciences of the United States of America (2018)

Neupert W. & Herrmann J.M. Translocation of proteins into mitochondria. Annual Review of Biochemistry 76, 723-749 (2007)

Peikert C.D., Mani J., Morgenstern M., Käser S., Knapp B., Wenger C., Harsman A., Oeljeklaus S., Schneider A. & Warscheid B. Charting organellar importomes by quantitative mass spectrometry. Nature Communications 8, article number 15272 (2017)

Schnaufer A., Clark-Walker G.D., Steinberg A.G. & Stuart K. The F1-ATP synthase complex in bloodstream stage trypanosomes has an unusual and essential function. The EMBO Journal 24(23), 4029-4040 (2005)

Schneider A., Bouzaidi-Tiali N., Chanez A.L. & Bulliard L. ATP production in isolated mitochondria of procyclic Trypanosoma brucei. Methods in Molecular Biology 372, 379-387 (2007)

Schneider A., Bursać D. & Lithgow T. The direct route: a simplified pathway for protein import into the mitochondrion of trypanosomes. Trends in Cell Biology 18(1), 12-8 (2008)

Schulz C., Schendzielorz A. & Rehling P. Unlocking the presequence import pathway. Trends in Cell Biology 25(5), 265-275 (2015)

Simarro P.P., Cecchi G., Paone M., Franco J.R., Diarra A., Ruiz J.A., Fèvre E.M., Courtin F., Mattioli R.C. & Jannin J.G. The Atlas of human African trypanosomiasis: a contribution to global mapping of neglected tropical diseases. International Journal for Health Geographics, 9-57 (2010)

Simarro P.P., Franco J.R., Cecchi G., Paone M., Diarra A., Ruiz Postigo J.A. & Jannin J.G. Human African trypanosomiasis in non-endemic countries (2000-2010). Journal of Travel Medicine 19(1), 44-53 (2011)

Smith T.K., Bringaud F., Nolan D.P. & Figueiredo L.M. Metabolic reprogramming during the *Trypanosoma brucei* life cycle [version 2; referees: 4 approved]. F1000Research 2017, 6(F1000 Faculty Rev):683

Šubrtová K, Panicucci B & Zíková A. ATPaseTb2, a unique membrane-bound FoF1-ATPase component, is essential in bloodstream and dyskinetoplastic trypanosomes. PLOS Pathogens 11(2), e1004660 (2015)

Raper J., Fung R., Ghiso J., Nussenzweig V. & Tomlinson S. Characterization of a novel trypanosome lytic factor from human serum. Infection and Immunity 67(4), 1910-1916 (1999)

Verner Z., Basu S., Benz C., Dixit S., Dobáková E., Faktorová D., Hashimi H., Horáková E., Huang Z., Paris Z., Peña-Diaz P., Ridlon L., Týč J., Wildridge D., Zíková A. & Lukeš J. Malleable mitochondrion of Trypanosoma brucei. International Review of Cell and Molecular Biology 315, 73-151 (2015)

Walker J.E. The ATP synthase: the understood, the uncertain and the unknown. Biochemical Society transactions 41(1), 1-16 (2013)

Zíková A., Schnaufer A., Dalley R.A., Panigrahi A.K. & Stuart K.D. The F_0F_1-ATP Synthase Complex Contains Novel Subunits and Is Essential for Procyclic *Trypanosoma brucei*. PLOS Pathogens 5 (2009)